



Charalampos Charalampidis, glaciologist  
Geological Survey of Denmark and Greenland (GEUS)  
Department of Earth Sciences, Uppsala University

Prof. dr. Edward Hanna  
Scientific editor  
The Cryosphere

J.nr. GEUS -  
Ref. -

Uppsala,  
18 October 2015

**Submission of revision: "Changing surface–atmosphere energy exchange and refreezing capacity of the lower accumulation area, west Greenland"**

Dear Prof. dr. Hanna,

We hereby submit our revised manuscript, initially submitted to The Cryosphere Discussions on 19 March 2015. The reviewers, while embracing our manuscript in its initial form, provided very valuable input towards its improvement. In response, we have performed changes, the most important of which we outline in the following:

We have tried to simplify the text throughout the manuscript in order to enhance the flow, and facilitate the reader towards our conclusions. The most significant changes are the exemplified paragraph in the review by Xavier Fettweis, and the last paragraph of our Discussion, where we removed the unnecessary quantifications and simply referred to the respective subsections in the Results. Also, an incorrect analysis at the "Melt-albedo feedback" subsection was identified and corrected (p. 2883, l. 20 of Discussion Paper), as the total amount of meltwater equals the sum of runoff and refreezing minus rainfall.

We have now clarified that the snow density in the simulations is the rounded measured density of snow-pit measurements in 2013. Also, in response to a very sharp comment by Xavier Fettweis, we have modified Table 4, and included the surface height changes. In the accumulation area, the permeable surface is a source of uncertainty for surface height monitoring, since during the melt season all objects tend to sink into the warmed snow and firn, following the percolation of meltwater. It is rather important for studies in the accumulation area to provide both surface height and mass budget estimates, and we are glad we were prompted to do so.

GEUS  
De Nationale Geologiske  
Undersøgelser for Danmark  
og Grønland  
Øster Voldgade 10  
1350 København K

Tlf. 38 14 20 00  
Fax 38 14 20 50

CVR-nr. 55 14 50 16  
EAN-nr. 5798000866003

geus@geus.dk  
www.geus.dk

*GEUS er en forsknings- og  
rådgivningsinstitution  
i Klima- og  
Energiministeriet*

We have removed all discussion of the North Atlantic Oscillation (NAO), because it is indeed a climatic aspect more relevant to studies of higher spatiotemporal scales. Our study reserves its conclusions even without the NAO, which indicates that its mention was unnecessarily high level of detail.

As suggested, we have also introduced a paragraph in the Discussion on the MODIS instrument sensitivity while referencing specialized studies on that matter (Wang et al., 2012; Lyapustin et al., 2014).

Further changes include an alternative reference for the PROMICE project (Ahlstrøm et al., 2008), as well as the citation of a paper describing our weather station setup (Citterio et al., 2015). A short comment about the uncertainty of refreezing estimates was also inserted in the introduction with the inclusion of a relevant citation (Vernon et al., 2013).

We should mention that two of our references are currently under review (Charalampidis et al., under review; Machguth et al., under review). However, we expect the editorial decision from their respective journals no later than the end of October this year.

Lastly – but more importantly – as you might have already noticed, we have decided to include Alun Hubbard and Samuel Doyle, as well as their current affiliations in the revised manuscript. Their contribution to our efforts is undeniable since throughout the years they have provided for the maintenance and logistical support of the KAN\_U weather station within the framework of the Greenland Analogue Project. We felt that the simple mention in the Acknowledgements of the Discussion Paper did not do justice to their contribution. They have welcomed our decision to include them as authors, and have kindly offered to proofread the study.

We look forward to your response. Don't hesitate to contact me if you have further questions.

Yours sincerely,

Charalampos Charalampidis

## References

Ahlstrøm, A. P. and the PROMICE project team: A new programme for monitoring the mass loss of the Greenland ice sheet, *Geol. Surv. Denmark Greenland Bull.*, 15, 61–64, 2008.

Charalampidis, C., van As, D., Colgan, W. T., Fausto, R. S., MacFerrin M., and Machguth H.: Thermal tracing of retained meltwater in the lower accumulation area of the southwestern Greenland ice sheet, *Ann. Glaciol.*, under review.

Citterio, M., van As, D., Ahlstrøm, A. P., Andersen, M. L., Andersen, S. B., Box, J. E., Charalampidis, C., Colgan, W. T., Fausto, R. S., Nielsen, S., and Veicherts, M.: Automatic weather stations for basic and applied glaciological research, *Geol. Surv. Denmark Greenland Bull.*, 33, 69–72, 2015.

Lyapustin, A., Wang, Y., Xiong, X., Meister, G., Platnick, S., Levy, R., Franz, B., Korkin, S., Hilker, T., Tucker, J., Hall, F., Sellers, P., Wu, A., and Angal, A.: Scientific impact of MODIS C5 calibration degradation and C6+ improvements, *Atmos. Meas. Tech.*, 7, 4353–4365, doi:10.5194/amt-7-4353-2014, 2014.

Machguth, H., MacFerrin, M., van As, D., Box, J. E., Charalampidis, C., Colgan, W. T., Fausto, R. S., Meijer, H. A. J., Mosley-Thompson, E. and van de Wal, R. S. W.: Greenland meltwater storage in firn limited by near-surface ice formation, *Nat. Clim. Change*, under review.

Vernon, C. L., Bamber, J. L., Box, J. E., van den Broeke, M. R., Fettweis, X., Hanna, E., and Huybrechts, P.: Surface mass balance model intercomparison for the Greenland ice sheet. *Cryosph.*, 7, 599–614, doi:10.5194/tc-7-599-2013, 2013.

Wang, D. D., Morton, D., Masek, J., Wu, A. A., Nagol, J., Xiong, X., Levy, R., Vermote, E., and Wolfe, R.: Impact of sensor degradation on the MODIS NDVI time series, *Remote Sens. Environ.*, 119, 55–61, doi:10.1016/j.rse.2011.12.001, 2012.

## Response to both reviewers

### Anonymous referee

*This is a very thorough analysis and interpretation of 5 years of automatic weather station data from the western flank of the Greenland Ice Sheet. The MS contains a wealth of meteorological data that will be of interest to other Greenland workers, and as such is worth publishing. There is also useful consideration of ice surface albedo feedback and sub-surface refreezing. I found the paper to be well-structured, well-written and -illustrated and easy to follow. I concur with many of the comments of Reviewer 1.*

### Referee Xavier Fettweis

*This paper presents recent changes in the energy balance and the snowpack behaviours at KAN\_U situated near the equilibrium line in the accumulation zone of the Greenland ice sheet. It is not the first time that energy balance and melt from in situ observations is discussed in this south-western part of the GrIS (van den Broeke et al., 2011) but KAN\_U is situated in the accumulation (while measurements from the ablation zone only was presented in van den Broeke et al. (2011)) and the discussion about the snowpack changes in 2012 is interesting, innovative and deserves to be published in TC with some minor revisions only.*

We thank Xavier Fettweis and an anonymous reviewer for their enthusiastic response, encouragement and constructive comments on our discussion paper. In the following, we address all points:

*The paper is clear and fits well with TC. The text is well written but sometimes it is hard to read due to the abundance of numbers and statistics in the text. Some simplifications when nothing important is told (e.g.: lines 1-10, pg 2883) could be made in the text by simply referencing to the corresponding tables.*

Taking also into account that Reviewer #2 found our discussion paper easy to follow, we have attempted some minor simplifications throughout the text, in order to make our quantifications more straightforward. The paragraph exemplified, we reformulated as: "Figure 9a, which depicts total monthly surface energy exchanges throughout the study period, illustrates that  $E_S^{\text{Net}}$  and  $E_L^{\text{Net}}$  dominate the SEB from May to September, while  $E_L^{\text{Net}}$  and  $E_H$  dominate the SEB during the remainder of the year. During the years exclusive of 2012 considered here (2009, 2010, 2011 and 2013), the total summer energy input to the ice sheet surface was 620–650 MJ m<sup>-2</sup>. This energy reaches a peak in July. In July 2010, for example, the total energy input reached 246 MJ m<sup>-2</sup>. By contrast, in 2012, the total summer energy input exceeded 770 MJ m<sup>-2</sup>, and in July it reached 304 MJ m<sup>-2</sup>. The 2012 total energy used for melt was 414 MJ m<sup>-2</sup> (65 % higher than in 2010), of which 183 MJ m<sup>-2</sup> was used for melt in July."

*Line 25, pg 2875 vs line 11 pg 2878: 360 or 400 kg/m3 for the snow density?*

Admittedly, it is an unclear wording. The measured average snow density is 360 kg m<sup>-3</sup>, used in Table 4 in the discussion paper. The snow density used in the simulations was rounded to 400 kg m<sup>-3</sup>. We have

reformulated as: “Solid precipitation is added in the model based on KAN\_U sonic ranger measurements, assuming the rounded average snow density found in snow-pit measurements, i.e. 400 kg m<sup>-3</sup>”.

*Table 4: I am a bit surprised that we use here a mean density of 360 Kg/m<sup>3</sup> for estimating the mean ablation rate. As snow is melting, the snowpack density should be higher.*

This is a fair point. Of course, there is density increase after melt percolates, as illustrated in Figures 9b and 11c of the discussion paper. We used this density in an attempt to estimate the mass flux melted for the first time from the initial snowpack each melt season. Arguably, this can be confusing, and not necessarily correct. Therefore, we decided to remove the estimated ablation rates from Table 4, as they are also not a crucial point in the study.

*Where does the density uncertainty of 40 kg/m<sup>3</sup> come from?*

This uncertainty is based on the standard deviation among the measurements from snow pit measurements conducted in spring 2013, which we now clarified in the caption.

*Just giving the difference in snow height is for me more reliable.*

Indeed, we also think that heights are more reliable and generally should be also provided, as SMBs are sometimes a matter of interpretation, especially in the accumulation area of the ice sheet. We have now inserted the winter/summer heights in Table 4. We did, however, keep also our SMB estimates for reference. The updated Table 4 of the discussion paper is shown here as Table I.

*Line 16, pg 2880: these low albedo values are for me more likely the result of the snowpack erosion by the wind (making apparent old firn) than reduced winter precipitation. The regional model MAR does not suggest particular low winter accumulation at KAN\_U in 2012-2013.*

We agree, and MAR is accurately suggesting substantial accumulation during winter 2012–2013 at KAN\_U. We also agree that there might have been snowpack erosion at our study site (Leanerts et al., 2014). However, this erosion is unlikely to have caused exposure of old firn. By November 2012, the snow thickness was 0.6 m (Fig. 2). From that point onward, and until spring 2013, the sonic ranger measurements suggest that there was limited accumulated snow on top of that initial snowpack in autumn; hence wind might have had an effect on surface, but certainly not erode the whole snowpack, thereby exposing firn. The snow at the surface probably lost part of its reflectivity after the prolonged exposure to the atmosphere. The area received substantial accumulation in spring. This was also verified by the Arctic Circle Traverse 2013 (ACT-13) in late April 2013, when we were at the location and the snow cover was ~ 0.9 m. After two weeks, the snow cover had increased by ~ 0.3 m.

*Lines 15-20, pg 2886: I do not see the interest of discussing NAO here. The role of NAO over Greenland is well known for explaining the recent melt increase and for me, Fig 10a as well as these 5 lines should be removed.*

Initially, our aim was to provide with a description as complete as possible, but we agree that information on the NAO, as well as its connection to recent climatic changes are readily available in the literature, and

perhaps more relevant to larger-scale studies. We have now removed all discussion of the NAO, and also Figure 10a. The new version of Figure 10 of the discussion paper is shown here as Figure 1.

*Lines 5-12, pg 2887: The comparison with MODIS is interesting but a part of the MODIS based albedo decrease could be the result of the declining instrument sensitivity of the MODIS sensors<sup>1</sup>. This issue should be discussed. However the same albedo trend is also simulated by MAR (forced by NCEP-NCARv1) which also simulates the exceptional low albedo in summer 2012 (see Fig.1 next page)!*

It is, indeed, an issue that should be mentioned when discussing remotely-sensed albedo. We have now included the following in the manuscript: “Part of the MODIS based albedo decrease could be the result of the declining instrument sensitivity of the Terra MODIS sensor (Wang et al. 2012; Lyapustin et al. 2014) though updated (through 2014) comparisons between MOD10A1 and ground observations from GC-Net data (Box et al. 2012; not shown) do not indicate an obvious nor statistically significant difference.”

*According to MAR, it is the first time in summer 2012 since 1950 that significant ice lenses appear but in 1960, MAR also simulates high runoff rates due to snowpack meltwater saturation suggesting that it is not the first time that significant melt events occur at Kan\_U.*

We have reasons to believe that this is partly incorrect. In detail, two firn cores were retrieved in May–June 1989 from Site J (66° 51.9' N, 46° 15.9' W, 2030 m a.s.l.; Kameda et al., 1995), ~ 36.2 km east-southeast from KAN\_U (Fig. 11a). According to the deduced Melt Feature Percentage (MFP) shown in Figure 11b (Kameda et al., 2004), 1960 has a higher melt feature percentage (MFP) than usual, but assuming that strong melt in 1960 would mostly percolate into previous year's firn layers, there is no indication that 1960 stands out much.

Another observational study analyses 10 m firn temperatures based on measurements prior to 1965 (Mock and Weeks, 1966). In their analysis, the closest site to KAN\_U was ~60 km south-southwest, i.e. at a lower elevation. According to this study, the estimated 10 m firn temperature at KAN\_U was at that time around –14 °C, suggesting that there was no significant refreezing in that period (and therefore ice content within the firn).

The above observations come from different settings, but they provide evidence from both higher and lower elevations than KAN\_U, thus bracketing out location. From these observations, we cannot explain the MAR-simulated meltwater at KAN\_U in 1959–1964 (Fig. 1 of the review) saturating the snowpack and not percolating to available pore space below. We believe this to be corroborated by the concurrent summer (JJA) albedo from MAR, the high values of which do not imply meltwater presence at the surface, but rather increased snow metamorphosis.

*Finally, while some runoff still occurs in 2013 (while the summer was cold) as a result of the 2012 summer induced snowpack compaction, runoff disappears in summer 2014 suggesting that we need several successive summers as 2012 to have a significant snowpack degradation.*

Correct, and a very good point. Hopefully, with the present study we communicated effectively that the years 2010–2011–2012 were three consecutive years of unusual atmospheric conditions that resulted in

negative net mass budgets and increased melt. The exceptional condition of the firn in 2012 was in part preconditioned by the two previous years. This can be understood by the analysis of the subsurface temperature measurements (Fig. 11a), and is the subject of another study (Charalampidis et al., under review). We should add at this point, that we are very pleased to see agreement on runoff between MAR and our results for the years 2012 and 2013.

*Some RACMO (or eventually MAR) outputs could be added in the manuscript to put the 2012 summer in a longer term perspective instead of using Kangerlussuaq measurements.*

A very good point, indeed. While in the present study we tried to base our argumentation exclusively on observations, it is our aim to increase the spatiotemporal perspective of our investigations using RCM output, which will be in fact the subject of a forthcoming study.

## References

- Charalampidis, C., van As, D., Colgan, W. T., Fausto, R. S., MacFerrin, M., and Machguth, H.: Thermal tracing of retained meltwater in the lower accumulation area of the southwestern Greenland ice sheet, *Annals of Glaciology*, under review.
- Kameda, T., Narita, H., Shoji, H., Nishio, F., Fujii, Y., and Watanabe, O.: Melt features in ice cores from Site J, southern Greenland: some implications for summer climate since AD 1550, *Annals of Glaciology*, 21, 51–58, 1995.
- Kameda, T., et al.: South Greenland Site J Ice Core Melt Percent and Temperature Reconstruction, IGBP PAGES/World Data Center for Paleoclimatology Data Contribution Series #2004-031, NOAA/NGDC Paleoclimatology Program, Boulder CO, USA, 2004.
- Lenaerts, J. T. M., Smeets, C. J. P. P., Nishimura, K., Eijkelboom, M., Boot, W., van den Broeke, M. R., and van de Berg, W. J.: Drifting snow measurements on the Greenland Ice Sheet and their application for model evaluation, *The Cryosphere*, 8, 801–814, doi:10.5194/tc-8-801-2014, 2014.
- Lyapustin, A., Wang, Y., Xiong, X., Meister, G., Platnick, S., Levy, R., Franz, B., Korkin, S., Hilker, T., Tucker, J., Hall, F., Sellers, P., Wu, A., and Angal, A.: Scientific impact of MODIS C5 calibration degradation and C6+ improvements, *Atmos. Meas. Tech.*, 7, 4353–4365, doi:10.5194/amt-7-4353-2014, 2014.
- Mock, S. J. and Weeks W. F.: The distribution of 10 meter snow temperatures on the Greenland 604 ice sheet, *J. Glaciol.*, 6, 23–41, 1966.
- Wang, D. D., Morton, D., Masek, J., Wu, A. A., Nagol, J., Xiong, X., Levy, R., Vermote, E., and Wolfe, R.: Impact of sensor degradation on the MODIS NDVI time series, *Remote Sens. Environ.*, 119, 55–61, doi:10.1016/j.rse.2011.12.001, 2012.

**Table I.** Surface height changes and mass budgets (measured in winter and calculated in summer) at KAN\_U in meters and m w.e., respectively, and ablation duration. The uncertainty of the surface height change is estimated at 0.2 m. The mass budgets are calculated assuming snow density of  $360 \text{ kg m}^{-3}$  (the average density of the uppermost 0.9 m measured on 26 April 2013), with uncertainty estimated at  $40 \text{ kg m}^{-3}$  (standard deviation among the snow-pit measurements). The snow density assumption was not needed in 2012 and 2013 when actual density measurements were conducted.

	winter height change	winter budget	summer height change	summer budget	net budget	ablation period
2008–2009	+1.64*	+0.59*±0.15	−0.71	−0.26±0.08	+0.34*±0.12	01/06–19/08
2009–2010	+0.70	+0.25±0.08	−1.22	−0.44±0.09	−0.19±0.12	30/04–05/09
2010–2011	+1.02	+0.37±0.08	−1.13	−0.41±0.09	−0.04±0.12	28/05–13/08
2011–2012**	+0.70	+0.25±0.08	−1.80	−0.86±0.14	−0.61±0.16	27/05–24/08
2012– 2013***	+1.24	+0.45±0.09	−0.75	−0.27±0.08	+0.18±0.12	29/05–17/08

\* value inferred from Van de Wal et al. (2012)

\*\* estimate based on snow-pit densities from May 2012

\*\*\* estimate based on snow-pit densities from May 2013



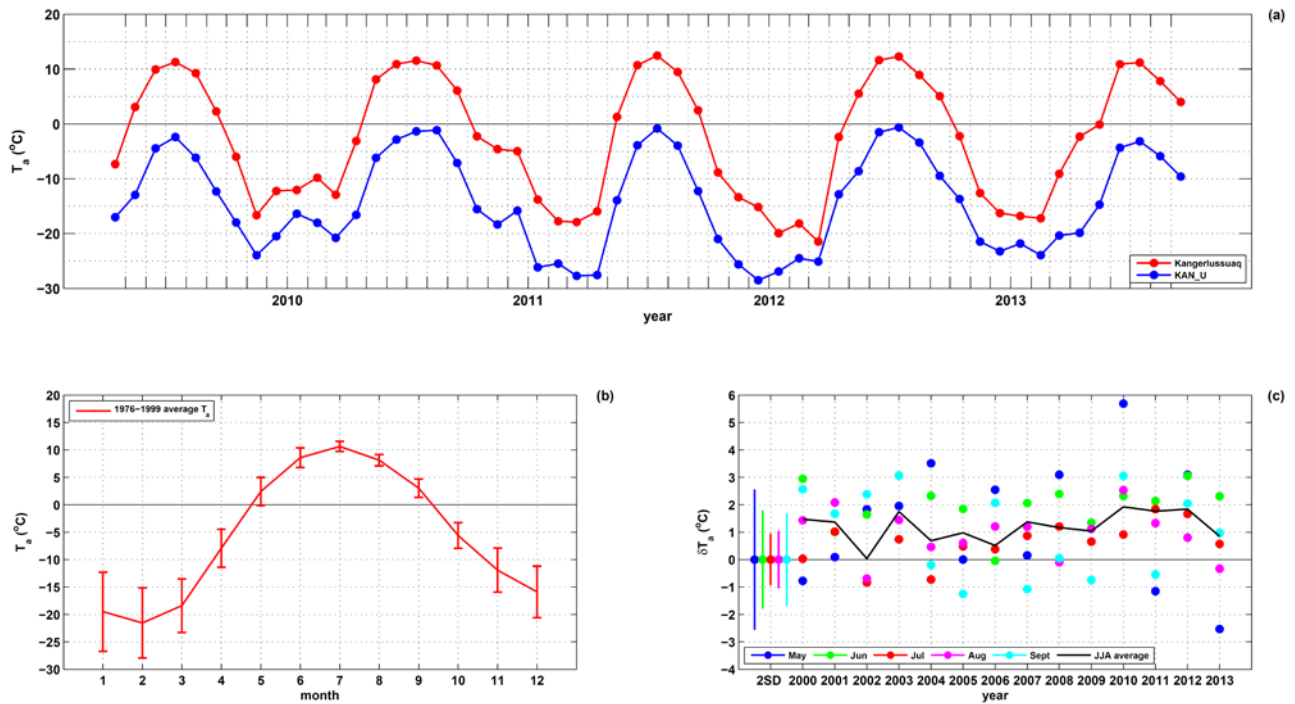


**Figure I. (a)** Monthly air temperature from Kangerlussuaq and at KAN U. Correlation coefficients: 0.97 for the extent of the KAN\_U data, 0.66–0.99 for the months individually, minimum being January. **(b)** Monthly reference period (1976–1999) air temperature at Kangerlussuaq. **(c)** Monthly (May to September) and summer (June-July-August average) air temperature anomalies at Kangerlussuaq for the years 2000–2013. Error bars indicate two standard deviations.

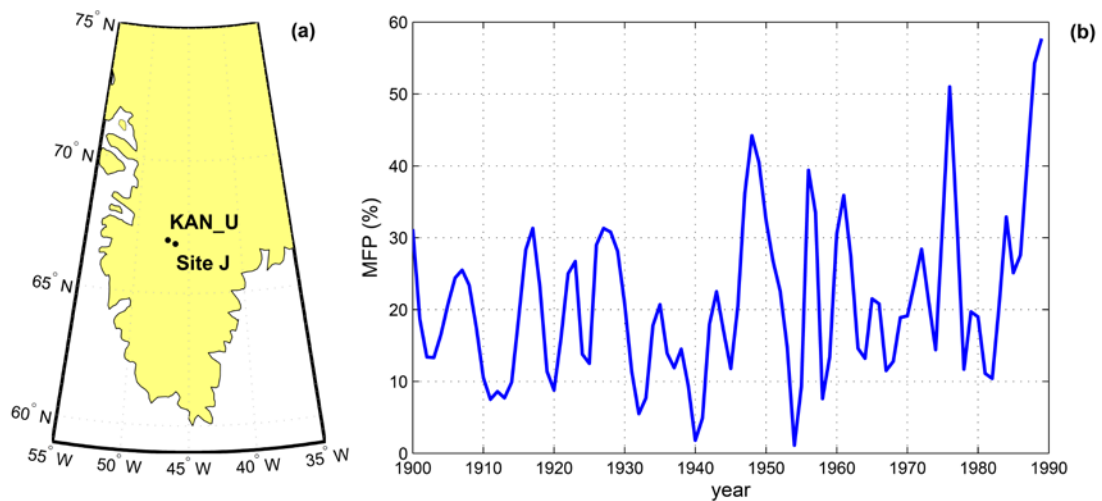


**Figure II. (a)** Location of Site J (Kameda et al., 1994) with respect to KAN\_U. **(b)** Melt percentage data from the top part of a firn core retrieved in 1989 at Site J by the Japanese Arctic Glaciological Expedition (JAGE89; Kameda et al., 2004).

1 **Changing surface-atmosphere energy exchange and**  
2 **refreezing capacity of the lower accumulation area, ~~west~~**  
3 **West Greenland**

4  
5 **C. Charalampidis<sup>1,2</sup>, D. van As<sup>1</sup>, J. E. Box<sup>1</sup>, M. R. van den Broeke<sup>3</sup>, W. T.**  
6 **Colgan<sup>1,4</sup>, [S. H. Doyle<sup>5</sup>](#), [A. L. Hubbard<sup>6</sup>](#), M. MacFerrin<sup>7,4</sup>, H. Machguth<sup>1,85</sup> and C. J.**  
7 **P. P. Smeets<sup>3</sup>**

8 [1]{Geological Survey of Denmark and Greenland (GEUS), Øster Voldgade 10, 1350,  
9 Copenhagen K, Denmark }

10 [2]{Department of Earth Sciences, Uppsala University, Villavägen 16, 752 36,  
11 Uppsala, Sweden }

12 [3]{Institute for Marine and Atmospheric research (IMAU), Utrecht University, P.O. Box  
13 80005, 3508TA, Utrecht, The Netherlands }

14 [\[4\]{Department of Earth and Space Sciences and Engineering, York University, 4700 Keele](#)  
15 [Street, M3J 1P3, Toronto, Canada}](#)

16 [\[5\]{Centre for Glaciology, Department of Geography and Earth Sciences, Aberystwyth](#)  
17 [University, Aberystwyth, SY23 3DB, United Kingdom}](#)

18 [\[6\]{Centre for Arctic Gas Hydrate, Environment and Climate, Department of Geology,](#)  
19 [University of Tromsø, Dramsveien 201, 9037, Tromsø, Norway}](#)

20 [\[74\]{Cooperative Institute for Research in Environmental Sciences \(CIRES\), 216 UCB,](#)  
21 [University of Colorado Boulder, Boulder, CO 80309, United States}](#)

22 [\[85\]{Arctic Technology Centre \(ARTEK\), Technical University of Denmark, Brovej, byg.](#)  
23 [118, 2800 Kgs. Lyngby, Denmark}](#)

24 Correspondence to: C. Charalampidis (cc@geus.dk)

25  
26 **Abstract**

27 We present five years (2009–2013) of automatic weather station measurements from the

28 | lower accumulation area (1840 m above sea level) of the Greenland ice sheet in the  
29 | Kangerlussuaq region, ~~western Greenland~~. Here, the summers of 2010 and 2012 were both  
30 | exceptionally warm, but only 2012 resulted in a strongly negative surface mass budget (SMB)  
31 | and surface meltwater runoff. The observed runoff was due to a large ice fraction in the upper  
32 | 10 m of firn that prevented meltwater from percolating to available pore volume below.  
33 | Analysis reveals an anomalously ~~relatively~~ low 2012 summer albedo of  $\sim 0.7$ , as meltwater  
34 | was present at the ice sheet surface. Consequently, during the 2012 melt season, the ice sheet  
35 | surface absorbed 28 % ( $213 \text{ MJ m}^{-2}$ ) more solar radiation than the average of all other years.

36 | A surface energy balance model is used to evaluate the seasonal and interannual variability of  
37 | all surface energy fluxes. The model reproduces the observed melt rates as well as the SMB  
38 | for each season. A sensitivity ~~test analysis~~ reveals that 71 % of the additional solar radiation  
39 | in 2012 was used for melt, corresponding to 36 % (0.64 m) of the 2012 surface lowering. The  
40 | remaining 1.14 m ~~of surface lowering resulted from~~ ~~was primarily due to the~~ high  
41 | atmospheric temperatures, up to  $+2.6 \text{ }^\circ\text{C}$  daily average, indicating that 2012 would have been  
42 | a negative SMB year at this site even without the melt-albedo feedback.

43 | Longer time series of SMB, regional temperature and remotely sensed albedo (MODIS) show  
44 | that 2012 was the first strongly negative SMB year, with the lowest albedo, at this elevation  
45 | on record. The warm conditions of ~~recent the last~~ years has resulted in enhanced melt and  
46 | reduction of the refreezing capacity ~~at-in~~ the lower accumulation area. If high temperatures  
47 | continue, the current lower accumulation area will turn into a region with superimposed ice in  
48 | coming years.

49

## 50 | 1 Introduction

51 | Glaciers and ice caps have dominated the cryospheric component to global average sea level  
52 | rise during the past century ( $0.5 \text{ mm yr}^{-1}$ , ~~i.e. or~~ about 70 % of the total cryospheric  
53 | component for the period 1961–2003; Solomon et al., 2007) due to their relatively short  
54 | response times to climate variability. However, the largest freshwater reservoir in the  
55 | Northern Hemisphere is the Greenland ice sheet, which would cause a sea level rise of 7.4 m  
56 | if completely melted (Bamber et al., 2013). The average sea level rise contribution from the  
57 | ice sheet has increased from  $0.09 \text{ mm yr}^{-1}$  over the period 1992–2001 to  $0.6 \text{ mm yr}^{-1}$  over the  
58 | period 2002–2011, according to the latest IPCC report (Vaughan et al., 2013). The sheer

59 volume of the ice sheet and the relatively large warming of the polar regions may yield an  
60 increasingly dominant contribution to cryospheric mass loss in coming decades.

61 An increasingly important driver of this accelerating mass loss is surface melt and subsequent  
62 runoff (Shepherd et al., 2012). Between 2009 and 2012, roughly 84% of the ~~increased~~  
63 Greenland ice sheet's ~~increased~~ mass loss was due to enhanced surface runoff ~~and reduced~~  
64 ~~SMB (Enderlin et al., 2014), causing a reduction of the surface mass budget~~~~SMB (SMB;~~  
65 ~~Ettema et al., 2009;~~ 2010; ~~Enderlin et al., 2014)~~. Increased melt is primarily the result of  
66 atmospheric warming (~~Huybrechts and de Wolde, 1999;~~ Huybrechts et al., 2011; ~~Huybrechts~~  
67 ~~and de Wolde, 1999)~~ and the darkening of the ice sheet (Bøggild et al., 2010; ~~Wientjes and~~  
68 ~~Oerlemans, 2010;~~ Box et al., 2012; Van As et al., 2013; ~~Wientjes and Oerlemans, 2010)~~. ~~It~~  
69 ~~has been postulated that the sea level rise associated with an~~ ~~An~~-increase in meltwater  
70 production ~~can be substantially buffered is commonly expected to be largely compensated for~~  
71 by water refreezing in snow and firn (Harper et al., 2012). However, it ~~has also been is~~  
72 suggested that ~~under in a~~-moderate warming ~~scenario~~-the ice sheet will lose 50% of its  
73 capacity to retain water by the end of the century (Van Angelen et al., 2013), ~~although there is~~  
74 ~~considerable uncertainty involved in retention estimates; based on SMB reconstructions~~  
75 ~~simulations (Vernon et al., 2013).~~

76 In-situ measurements are essential for understanding the impact of the changing atmospheric  
77 conditions on the ice sheet. In the Kangerlussuaq region, West Greenland, seven automatic  
78 weather stations (AWS) and nine SMB stakes constitute a relatively dense network of in-situ  
79 measurements (Van de Wal et al., 1995; Greuell et al., 2001; Van den Broeke et al., 2008a;  
80 Van As et al., 2012). The uppermost AWS, KAN\_U, was established on 4 April 2009 (67° 0'  
81 0" N, 47° 1' 1" W; Fig. 1). Located approximately 140 km inland from the ice margin and at  
82 about 1840 m above sea level (a.s.l.), KAN\_U is one of the few AWS in Greenland located in  
83 the lower accumulation area, where small changes in climate forcing will ~~likely~~ have the  
84 largest impact on ~~the~~-ice sheet ~~near-surface~~ ~~stratigraphy~~.

85 In the Kangerlussuaq region, approximately 150 km of mountainous tundra separates the ice  
86 sheet from the ocean. Characteristic for the ice sheet in this region is a relatively wide  
87 (approx. 100 km) ablation area. The equilibrium line altitude (ELA), where annual  
88 accumulation and ablation are equal, was estimated to be 1535 m a.s.l. for the period of 1990–  
89 2003 (Van de Wal et al., 2005), but is reported to have increased ~~to~~ ~~(~~1533 m a.s.l. for ~~the~~

90 ~~period of~~ 1990–2011 (~~;~~ Van de Wal et al., 2012). At 1520 m a.s.l., superimposed ice becomes  
91 ~~apparent-evident~~ at the [ice sheet](#) surface at the end of every ablation season, and its upglacier  
92 extent is estimated ~~until-to reach~~ about 1750 m a.s.l. (Van den Broeke et al., 2008a). The  
93 percolation area is found at higher elevations, up to about 2500 m a.s.l., ~~which is~~ the lower  
94 limit of the dry snow area.

95 The ablation area in this region has been studied extensively. Van den Broeke et al. (2008a)  
96 presented four years of radiation measurements below the ELA. The lowest albedo values are  
97 found at the intermediate AWS S6 (1020 m a.s.l.) due to ~~a the surface melt water induced~~  
98 "dark band" ~~induced by surface meltwater~~ (Greuell, 2000; Wientjes and Oerlemans, 2010).  
99 Melt modelling revealed ~~an the increase of-in~~ summer melt toward the margin, and ~~the-a~~  
100 ~~decrease in decreasing role of~~ sensible heat flux with increasing elevation, but also ~~the-an~~  
101 ~~increasing in the importance dominance~~ of shortwave radiation in the surface energy balance  
102 (SEB) during melt at higher elevations (Van den Broeke et al., 2008b; 2011). An annual  
103 cycle in surface roughness length ~~was-has been~~ found to exist over a large part of the ablation  
104 area (Smeets and van den Broeke, 2008). This determines part of the variability in the  
105 turbulent heat fluxes during the summer months (~~as-presented-by~~ Van den Broeke et al.,  
106 ~~(2009)~~). This ~~latter~~ study showed that the ~~regional~~ katabatic ~~nature-of-the-winds-over-the~~  
107 ~~region~~, in combination with the variable surface roughness ~~in-at the-lower~~ ~~regionselevations~~,  
108 provides significant year-round turbulent heat transfer in a stable surface layer. An increasing  
109 wind speed with surface elevation was identified, contrary to what would be expected from  
110 katabatically forced wind over an ice surface flattening with elevation. This is due to the  
111 larger surface roughness near the margin (Smeets and van den Broeke, 2008), the increasing  
112 influence of the large scale pressure gradient force (Van Angelen et al., 2011) and the  
113 proximity of pooled cold air over the tundra that sets up an opposing pressure gradient force  
114 in the boundary layer during winter. Van As et al. (2012) quantified the extreme surface melt  
115 in the Kangerlussuaq region in 2010, validated by river discharge measurements.

116 At elevations above the superimposed ice area and below the dry snow area (i.e. ~1750–2500  
117 m a.s.l.), sufficient melt occurs to impact snow/firn properties, but not enough to reveal bare  
118 ice. In a warming climate with melt ~~at-increasingly occurring at~~ higher elevations, this area  
119 would comprise an increasingly large portion of the ice sheet due to the ice sheet's flattening  
120 with increasing elevation (~~McGrath et al., 2013~~). A rare event in July 2012 caused melt at all  
121 elevations of the ice sheet (Nghiem et al., 2012). Bennartz et al. (2013) ~~partially~~ attributed this

122 | Greenland-wide event of increased near-surface temperatures ~~partially~~ to thin, low-level  
123 | liquid clouds. These clouds, while optically thick and low enough to enhance downward  
124 | longwave radiation, were thin enough for solar radiation to reach the [ice sheet](#) surface. They  
125 | were present at Summit station about 30% of the time during the 2012 summer months.

126 | A large difference ~~between with~~ the ablation and accumulation areas is that in the  
127 | accumulation area, processes within the snow/firn layers, such as meltwater percolation and  
128 | refreezing, significantly impact the mass budget (Harper et al., 2012). Additionally, an  
129 | important process is the melt-albedo feedback (Box et al., 2012). Our aim is to assess ~~the~~  
130 | SMB sensitivity to atmospheric forcing in the lower accumulation area using AWS  
131 | measurements that serve as input for a SEB model. The five-year period with AWS  
132 | measurements (2009–2013) spans a wide range of melting conditions, including the record  
133 | melting years of 2010 and 2012 (Tedesco et al., 2011; 2013; Van As et al., 2012; Nghiem et  
134 | al., 2012; Hanna et al. 2014) and years with limited melting such as 2009 and 2013. We add  
135 | temporal perspective by discussing Kangerlussuaq temperatures since 1976 and Moderate  
136 | Resolution Imaging Spectroradiometer (MODIS) albedo values since 2000. ~~In the~~  
137 | ~~following~~ [Below](#), we first describe the observations and SEB calculations, after which we ~~will~~  
138 | present ~~the~~ atmospheric conditions and surface energy fluxes at KAN\_U, and the changes  
139 | therein due to recent years with extreme melt. Finally, we investigate the importance of the  
140 | melt-albedo feedback on the SMB of the lower accumulation area and discuss how changes in  
141 | the firn can yield SMB variability on ~~an short~~ interannual time scale.

142

## 143 | **2 Methods**

### 144 | **2.1 AWS measurements**

145 | KAN\_U is part of the ~~network of~~ ~20 AWSs comprising in the Programme for Monitoring of  
146 | the Greenland Ice Sheet (PROMICE) network (~~;~~ Ahlstrøm et al., ~~2011~~2008). Measurements  
147 | include ambient air pressure, relative humidity and aspirated temperature ( $T_a$ ) at 2.7 m height  
148 | above [the ice sheet](#) surface, wind speed and direction at 3.1 m height, as well as incoming and  
149 | reflected solar/shortwave ( $E_S^\downarrow$ ,  $E_S^\uparrow$ ) and downward and emitted terrestrial/longwave ( $E_L^\downarrow$ ,  $E_L^\uparrow$ )  
150 | radiation components at 10-minute intervals. Accumulation and ablation are measured by two  
151 | sonic rangiers, one attached to the AWS and one on a separate stake assembly (Fig. 1b).

152 Sensor specifications are listed in Table 1. The AWS transmits hourly measurements during  
153 the summer period and daily during winter ([Citterio et al., 2015](#)).

154 AWSs installed on glaciers are prone to tilt due to ~~the transient changes evolution of~~ the ice  
155 or firn surface. The importance of accounting for ~~the~~ pyranometer tilt has been discussed by  
156 ~~e.g.~~ MacWhorter and Weller (1991). AWSs located in accumulation areas are comparatively  
157 stable due to the accumulated snow on the base of the tripod. The maximum tilt registered by  
158 KAN\_U is 3.0 degrees. A tilt correction for the solar radiation measurements is made after  
159 Van As (2011).

160 Two gaps in (sub) ~~hourly~~ hourly measurements exist due to a malfunctioning memory card,  
161 from 27 October 2010 until 22 April 2011 and from 26 October 2011 until 21 January 2012.  
162 During these periods, ~~when~~ ~~with~~ only transmitted daily values are available, measurements  
163 from a second AWS, ~~S10~~, erected on 17 August 2010 at ~50 m distance from KAN\_U, were  
164 used ~~and~~, adjusted by linear regression to eliminate systematic prevent e.g. offset\_s due to a  
165 different ~~ee in~~ measurement heights. The overlapping ~~time series records~~ of the two time series  
166 revealed high cross-correlations and low ~~Rootroot-Meanmean-Square-squared\_Deviations~~  
167 deviations (RMSD) for every measured parameter (Table 2). Due to technical issues with  
168 S10,  $E_L^\downarrow$ ,  $E_L^\uparrow$  and  $T_a$  measurement gaps from 9 February 2011 until 30 April 2012 were filled  
169 with a similar approach, using measurements from AWS S9 located 53 km closer to the ice  
170 sheet margin. Any added uncertainty from using adjusted wintertime measurements will have  
171 minimal impact on the summertime results presented below.

172 The broadband albedo is the fraction of the incoming shortwave radiation reflected at the ice  
173 sheet surface and an important parameter in studying the changes in the accumulation area:

$$174 \quad \alpha = \left| \frac{E_s^\uparrow}{E_s^\downarrow} \right| \quad (1)$$

175 To verify its accuracy, albedo was compared for both AWSs KAN\_U and S10 for the warm  
176 seasons (May–September) of 2010, 2011 and 2012 (Table 2). For hourly values, the RMSD  
177 for 2010 and 2011 was only ~0.03. The RMSD for 2012 was 0.07, due to the larger-higher  
178 spatial variability in surface reflectance after substantial melt.



## 179 2.2 Surface radiation budget

180 The radiation budget at the [ice sheet](#) surface is given by the sum of solar and terrestrial  
181 radiation components:

$$182 E_{\mathbf{R}} = E_S^{\downarrow} + E_S^{\uparrow} + E_L^{\downarrow} + E_L^{\uparrow} = E_S^{\text{Net}} + E_L^{\text{Net}} \quad (2)$$

183 Fluxes are here taken as positive when directed toward the [ice sheet](#) surface. By the inclusion  
184 of albedo and utilizing the Stefan-Boltzmann law, this can be rewritten as:

$$185 E_{\mathbf{R}} = (1 - \alpha) E_S^{\downarrow} + \varepsilon E_L^{\downarrow} - \varepsilon \sigma T_S^4 \quad (3)$$

186 with  $\sigma$  being the Stefan-Boltzmann constant ( $5.67 \times 10^{-8} \text{ W m}^{-2} \text{ K}^{-4}$ ) and  $T_S$  the surface  
187 temperature. The longwave emissivity  $\varepsilon$  for snow/ice is assumed equal to 1 (black-body  
188 assumption).

## 189 2.3 SEB model

190 Various studies have applied SEB models in glaciated areas under different climatic  
191 conditions, [such as a \(e.g. high Antarctic plateau \(Van As et al., 2005\) and the ; Greenland](#)  
192 [ablation area \(Van den Broeke et al., 2008b; 2011\)](#). The energy balance at the atmosphere-  
193 surface interface is:

$$194 E_M = E_{\mathbf{R}} + E_H + E_E + E_G + E_P \quad (4)$$

195 where  $E_H$ ,  $E_E$ ,  $E_G$  and  $E_P$  are the turbulent sensible, turbulent latent, subsurface conductive  
196 and rain-induced energy fluxes, respectively.

197 Rainfall is assumed to be at melting-point temperature ( $T_0 = 273.15 \text{ K}$ ), thus  $E_P$  is non-zero  
198 when  $T_s$  is below freezing:

$$199 E_P = \rho_w c_w \dot{r} (T_0 - T_s) \quad (5)$$

200 where  $c_w$  is the specific heat of water ( $4.21 \text{ kJ kg}^{-1} \text{ K}^{-1}$  at  $0^\circ\text{C}$  [and  \$999.84 \text{ kg m}^{-3}\$](#) ) and  $\dot{r}$  is the  
201 rainfall rate. The latter is assumed [to be](#) non-zero [when-under](#) conditions of heavy cloud cover  
202 during periods with non-freezing air temperatures [are met](#) (see below).

203 The energy balance is solved for the one unknown variable  $T_s$ . If  $T_s$  is limited to the melting-



204 point temperature (273.15 K), the imbalance in Eq. 4 is attributed to melt ( $E_M$ ). For sub-  
205 freezing  $T_s$  values all other SEB components are in balance and surface melt does not occur.  
206  $E_H$  and  $E_E$  are calculated using the “bulk method” as described by Van As et al. (2005). This  
207 method uses atmospheric stability, and thus depends on  $T_s$ , implying that Eq. 4 has to be  
208 solved iteratively.

209 The average surface roughness length for momentum  $z_0$  at this elevation would realistically be  
210  $\sim 10^{-4}$  m (Smeets and van den Broeke, 2008). During summer, the [ice sheet](#) surface melts  
211 occasionally, smoothing it and thus attaining a smaller  $z_0$  ( $\sim 10^{-5}$  m). Slightly increased  
212 roughness is expected during wintertime due to sastrugi and drifting snow ([Lenaerts et al.,](#)  
213 [2014](#)) can increase  $z_0$  in cases up to  $10^{-3}$  m ([Lenaerts et al., 2014](#)). In the present study,  $z_0$  is  
214 kept constant at  $10^{-4}$  m. A series of test runs showed that the results of this study were not  
215 very sensitive ~~to in~~ the range of plausible  $z_0$  values. The scalar roughness lengths for heat and  
216 moisture are calculated according to Andreas (1987).

217 Subsurface heat transfer is calculated on a 200-layer grid with 0.1 m spacing (20 m total) and  
218 is forced by temperature changes at the surface and latent heat release when water refreezes  
219 within the firn. Heat conduction is calculated using effective conductivity as a function of firn  
220 density (Sturm et al., 1997) and specific heat of firn as a function of temperature (Yen, 1981).  
221 The calculations are initialized using thermistor string temperatures from April 2009 and  
222 depth-adjusted firn core densities measured on 2 May 2012. The subsurface part of the model  
223 includes a percolation/refreezing scheme based on Illangasekare et al. (1990), assuming active  
224 percolation within snow/firn. Provided that there is production of meltwater at the surface, the  
225 amount of refreezing is limited either by the available pore volume or by the available cold  
226 content at each level. The scheme simulates water transport and subsequent refreezing as the  
227 progression of a uniform warming front into the snow/firn and is active for all melt seasons  
228 except for 2012. In 2012, surface runoff dominated ~~ds~~ water movement after 14 July, as clearly  
229 visible on Landsat imagery (not shown). This coincided with the surfacing of a 6 m thick ice  
230 layer in the model, which was also found in firn cores (Machguth et al., under review).  
231 ~~Consistent with these observations, Here~~ we use 6 m of ice (density of  $900 \text{ kg m}^{-3}$ ) as a  
232 threshold that causes meltwater to run off horizontally, shutting down vertical percolation.

233 [Solid precipitation is added in the model based on KAN U sonic ranger measurements,](#)  
234 [assuming ~~the~~ a rounded average snow density of  \$400 \text{ kg m}^{-3}\$  observed found in snow-pit](#)

235 ~~measurements, i.e.  $400 \text{ kg m}^{-3}$~~  Solid precipitation is added in the model based on KAN\_U  
236 ~~sonic ranger measurements, assuming snow density of  $400 \text{ kg m}^{-3}$  in accordance to snow pit~~  
237 ~~measurements~~. Although rain occurs ~~only sporadically infrequently~~ at 1840 m a.s.l., a rain  
238 estimate is incorporated with prescribed precipitation rates for each year during hours with a  
239 thick cloud cover producing  $E_L^\downarrow$  values that exceed black-body radiation using the air  
240 temperature ( $E_L^\downarrow > \sigma T_a^4$ ) and  $T_a$  is above freezing. ~~Testing-Evaluating~~ this against winter  
241 accumulation, the following precipitation rates were ~~found-derived~~ and ~~applied-prescribed~~ to  
242 the rain calculation:  $2.0 \times 10^{-3} \text{ m h}^{-1}$  for 2009–2010 and 2012–2013,  $3.5 \times 10^{-3} \text{ m h}^{-1}$  for  
243 2010–2011 and  $0.5 \times 10^{-3} \text{ m h}^{-1}$  for 2011–2012. Using this approach, the model produces  
244 liquid precipitation during the summer months only; by the end of the five-year period it  
245 amounts to a total of 0.26 m ~~water equivalent (m w.e.)~~, 15% of the total precipitation over the  
246 five years. The contribution of rain in the energy balance is minor; the total energy added to  
247 the surface for the whole study period is approximately  $1.15 \text{ MJ m}^{-2}$ , which could yield a total  
248 of 9 mm of melted snow.

249 The performance of the model in terms of ablation is illustrated by comparing ~~the~~ simulated  
250 ~~surface changes~~ with the measured surface height changes due to ablation and accumulation  
251 ~~in~~ (Fig. 2a). The model accurately reproduces the melt rates during every melt season. Yet  
252 this validation does not cover the whole melt season. We found that the AWS tripod and stake  
253 assembly are prone to sinking somewhat into warm, melting firn during the second part of the  
254 melt season (note the measurement gaps). In a second model validation ~~method-exercise~~, we  
255 compare ~~the~~ simulated ~~and with the~~ measured  $T_s$  (inferred from the  $E_L^\uparrow$ ) in Fig. 2b, and find  
256 they correlate well ( $R^2 = 0.98$ ) with an average difference of  $0.11 \text{ }^\circ\text{C}$  and ~~Rootroot-~~  
257 ~~Meanmean-Square-squared Error-error~~ (RMSE) of  $1.43 \text{ }^\circ\text{C}$ . Part of ~~this~~ difference can be  
258 attributed to the seemingly overestimated 10%  $E_L^\uparrow$  measurement uncertainty as reported by  
259 the sensor manufacturer, which would yield a RMSE of  $6.2 \text{ }^\circ\text{C}$  of  $T_s$  values.

## 260 2.4 Additional measurements

261 For a study with a five-year time span, it is useful to provide a longer temporal perspective.  
262 For this, ~~we use North Atlantic Oscillation (NAO) index measurements from the National~~  
263 ~~Oceanic and Atmospheric Administration (NOAA)~~. We use the air temperature record from  
264 Kangerlussuaq airport ~~observed~~ by the Danish Meteorological Institute (DMI) ~~since, initiated~~  
265 ~~in~~ 1973 ~~in support of to facilitate aircraft flight~~ operations (Cappelen, 2013). Full

266 | observational suite coverage is available ~~from~~ since 1976. Monthly  $T_a$  from the airport  
267 | correlate well with the KAN\_U time series ( $R = 0.97$ ), indicating that Kangerlussuaq  
268 | measurements can be used for providing temporal perspective, ~~despite~~ in spite of the 160 km  
269 | distance that separates the two measurement sites. Finally, ~~from~~ we ~~5x5 km~~ regridded  
270 | ~~MODIS albedo measurements (MOD10A1)~~ we use the pixel nearest to KAN\_U in 5 by 5 km  
271 | regridded MODIS albedo product (MOD10A1) to investigate albedo variability over ~~in a~~ the  
272 | 2000–2013 perspective ~~period~~.

273

## 274 | **3 Results**

### 275 | **3.1 Meteorological observations**

276 | The importance of katabatic and synoptic forcing on near-surface wind direction ~~is~~ are  
277 | roughly equivalent ~~equally important~~ at the elevation of KAN\_U (Van Angelen et al., 2011).  
278 | The average wind direction is south-southeast ( $\sim 150^\circ$ ; Fig. 3a). ~~Yet~~ However, in a case study  
279 | of the 2012/2013 winter (Van As et al., 2014), the prevailing wind direction ~~of~~ was  $\sim 135^\circ$   
280 | (southeast), suggesting an influential katabatic regime in which air drains down-slope and is,  
281 | deflected by the Coriolis ~~foreing~~ Effect. Wind speed is higher during winter (Fig. 3b); annual  
282 | average values are 6–7  $\text{m s}^{-1}$ , whereas summer average values are around 5  $\text{m s}^{-1}$  (Table 3).  
283 | Winds exceeding 15  $\text{m s}^{-1}$  occur primarily during the winter period and rarely exceed 20  $\text{m s}^{-1}$   
284 | when averaged over 24 hours. The barometric pressure of about 800 hPa exhibits an annual  
285 | cycle with relatively high pressure in summer (Fig. 3c), favoring more stable, clear-sky  
286 | conditions. Also the specific humidity varies annually, peaking in summer. Annual values are  
287 | about 1.5  $\text{g kg}^{-1}$ .

288 | The year 2010 was the warmest year of the record (Table 3), with the winter (December-  
289 | January-February) of 2009–2010 being 4.0  $^\circ\text{C}$  warmer than the 2009–2013 average, and the  
290 | summer (June-July-August) only being equaled by 2012 ( $-1.8^\circ\text{C}$ ; Table 3). ~~Especially~~ May  
291 | 2010 was especially warm, at  $-6.2^\circ\text{C}$ , or  $5.1^\circ\text{C}$  above the 2009–2013 average. Positive  $T_a$   
292 | persisted during the end of the melt season resulting in a  $-1.1^\circ\text{C}$  monthly average for August.  
293 | The high 2010 temperatures influenced ~~impacted the~~ surface ablation by inducing early  
294 | onset. In 2010, ablation, ~~which~~ lasted from late April until early September, whereas, for  
295 | instance, the 2009 melt season at KAN\_U ~~occurred~~ spanned early June until mid-August.

296 The average SMB over the period 1994–2010 at KAN\_U is +0.27 m w.e. (Van de Wal et al.,  
297 2012). Melt at this elevation occurs ~~frequently~~ during each melt season. The winter 2009/  
298 2010 accumulation was relatively low, amounting to 65% of the 2009–2013 average (0.25 m  
299 w.e.; Table 4). During the 2010 melt season, all the ~~snow that had~~ accumulated ~~snow~~ since the  
300 end of the previous melt season ablated, including part of the underlying firn, resulting in the  
301 first negative SMB year on record (Table 4). The stake measurements from Van de Wal et al.  
302 (2012) document a two-year surface height change of +0.42 m on average for 2008–2010 at  
303 the same location (S10), corresponding to +0.15 m w.e. assuming a snow pit density of 360  
304 kg m<sup>-3</sup>. From this estimate, we infer the winter and net SMB for 2009 to be +0.59 and +0.34  
305 m w.e., respectively.

306 During winter 2011–/2012, accumulation was ~~the same~~ similar as in winter 2009–/2010. In  
307 spring 2012, positive  $T_a$  was first recorded during April (with –12.8 °C the warmest April on  
308 record), followed by a relatively warm May (–8.6 °C). Already in late May 2012 ablation  
309 rates were high (7.2 mm w.e. d<sup>-1</sup>; Charalampidis and van As, 2015in press). June and July  
310 were the warmest of the five-year record with –1.5 °C and –0.6 °C monthly average  $T_a$ ,  
311 respectively. With the summer of 2012 on average as warm as that of 2010, but the ablation  
312 period shorter by 398 days (Table 4), the summer SMB was –0.86 m w.e., making 2012 ~~the~~  
313 ~~most a~~-strongly negative SMB year (–0.61 m w.e.) to be recorded at this location (Van de Wal  
314 et al., 2005; 2012).

### 315 3.2 Surface energy fluxes

316 Solar radiation exhibits a strong annual cycle at this location ~~above ion~~ the ~~Arctic C~~polar  
317 ~~circle~~ (Fig. 4a). In the absence of topographic shading or a significant surface slope (~0.37°)  
318 the day-to-day variability in incoming shortwave radiation at this elevation is dominated by  
319 cloudiness and the solar zenith angle. The highest daily  $E_S^\downarrow$  values occur in June and exceed  
320 400 W m<sup>-2</sup>, while at the ELA they are just below 400 W m<sup>-2</sup> (Van den Broeke et al., 2008a)  
321 due to more frequent cloud cover and a thicker overlying atmosphere. Whereas  $E_S^\downarrow$  increases  
322 with elevation from the ELA to KAN\_U,  $E_S^{\text{Net}}$  obtains values of up to 100 W m<sup>-2</sup> both at the  
323 ELA and at KAN\_U, implying ~~regulated~~ solar energy input ~~that is regulated~~ by surface  
324 reflectance.

325 Terrestrial radiation exhibits an annual cycle of smaller amplitude (Fig. 4a). The annual

326 variations of the downward and emitted longwave radiation are governed by the temperature  
327 and emissivity variations of the atmosphere and the [ice sheet](#) surface, respectively. Hence, the  
328 absolute magnitudes of both components are larger during the summer period.  $E_L^\downarrow$   
329 fluctuations depend primarily on cloud cover.  $E_L^\uparrow$  is a sink to the SEB and during summer is  
330 limited by the melting surface with the maximum energy loss being  $316 \text{ W m}^{-2}$ . This results  
331 in predominantly negative  $E_L^{\text{Net}}$  values throughout the year. The energy loss peaks during  
332 June and July.

333 The  $E_R$  annual cycle displays an energy gain at the [ice sheet](#) surface during May to August  
334 and energy loss the rest of the year (Fig. 4b). This winter energy loss is primarily  
335 compensated by downward sensible heat flux. Calculated  $E_H$  is typically positive throughout  
336 the year, with highest values in winter when  $E_R$  is most negative, heating the [ice sheet](#) surface  
337 while cooling the atmospheric boundary layer (Fig 4b). This facilitates the katabatic forcing  
338 and thus enhances wind speed and further turbulent energy exchange between the atmosphere  
339 and [the ice sheet](#) surface. The contribution of  $E_H$  to melt is smaller than at lower elevations  
340 (Van den Broeke et al., 2011). ~~T;~~ the dominant melt energy source at KAN\_U is  $E_R$ .

341  $E_E$  changes sign from winter to summer, and is on average a small contributor to the annual  
342 SEB. During the summer period,  $E_E$  is comparable to  $E_H$  but with opposite sign, enabling  
343 surface cooling by sublimation and/or evaporation. In the winter,  $E_E$  is directed mostly toward  
344 the cold [ice sheet](#) surface, resulting in heating from deposition.

345 The annually averaged  $E_G$  is mostly negative and of the same magnitude as  $E_E$  ( $3\text{--}4 \text{ W m}^{-2}$ ),  
346 but with no distinct annual cycle. Melt seasons with substantial refreezing exhibit increased  
347 positive summer-averaged  $E_G$  since the near-surface firn temperature is on average higher  
348 than  $T_s$ , leading to conductive heat transport toward the [ice sheet](#) surface. Low  $E_G$  values in  
349 summer indicate limited refreezing in the firn just below the [ice sheet](#) surface.

350  $E_P$  is non-zero, but still negligible in summer, when positive air temperatures occur and thus  
351 precipitation is liquid.

### 352 **3.3 Interannual variability of the SEB and implications for melt**

353 With the exception of August 2009, when predominantly clear skies caused  $E_S^\downarrow$  being  $40 \text{ W}$   
354  $\text{m}^{-2}$  larger, and  $E_L^\downarrow$   $36 \text{ W m}^{-2}$  smaller, than in the other years, monthly average values of  $E_S^\downarrow$

355 at this site are fairly invariant (difference  $< 25 \text{ W m}^{-2}$ ; Fig. 5a). Often  $E_R$  increases when  
356 clouds are present over an ice sheet; a so-called radiation paradox (Ambach, 1974), as it was  
357 observed in April 2012.

358 Figure 5b illustrates the annual cycle of monthly average albedo, not including the winter  
359 months October–February, when shortwave radiation values are too low for accurate albedo  
360 estimation, yet it is expected to ~~be characteristic of attain~~ fresh dry snow values (0.8–0.9).  
361 High albedo persists until May due to fresh snow depositeds on the ice sheet surface. An  
362 exception occurred during March and April 2013, when the monthly albedo of 0.78 suggests  
363 reduced precipitation input for a prolonged period and the presence of ~~aging old, clean, dry~~  
364 snow on the ice sheet surface (Cuffey and Paterson, 2010). In the years 2009–2011 and 2013  
365 the albedo gradually decreased beginning late May and during the summer due to the effects  
366 of relatively high temperatures and melt on snow metamorphism. During summer, albedo still  
367 exceeded 0.75. While in August melt at KAN\_U can still occur, this does not counteract the  
368 effect of snowfall events that increase the surface albedo.

369 The anomalously warm period in June and July 2012 (Fig. 3d) coincided with a larger  
370 decrease ~~of in~~ surface albedo than in the other years. The combination of enhanced melting,  
371 heat-induced metamorphosis and firn saturation, reduced the albedo from 0.85 in April to 0.67  
372 in July reaching a value that ~~is characteristic of corresponds to the lower~~ soaked snow facies  
373 close to the lower elevation snow/firn line (Cuffey and Paterson, 2010). As a consequence,  
374  $E_S^{\text{Net}}$  increased by approximately  $25 \text{ W m}^{-2}$  in June and July (32%; Fig. 5c). This darkening  
375 thus functions as an amplifier of melt (Box et al., 2012; Van As et al., 2013), contributing to  
376 the large observed ablation ~~rates~~ (Table 4).

377 The largest longwave radiation surface emissions occurred during August 2010 and June–July  
378 2012, approaching the theoretical limit of  $-316 \text{ W m}^{-2}$  for a continuously melting ice sheet  
379 surface (Fig. 6b). The concurrent high  $E_L^\downarrow$  (Fig. 6a; Table 5) was related to high atmospheric  
380 temperatures. This caused summer  $E_L^{\text{Net}}$  in ~~the summers~~ 2010 and 2012 to exceed its value in  
381 other years (Table 5; Van As et al., 2012). While summer  $E_S^{\text{Net}}$  was similar in 2009 and 2010,  
382 summer  $E_R$  was ~~about 690%~~ larger in 2010 than in 2009, primarily due to the high  
383 atmospheric temperatures ~~alone~~. During ~~summer~~ 2012, summer  $E_L^{\text{Net}}$  was similar as in 2010.  
384 The large summer  $E_S^{\text{Net}}$ , resulted in summer  $E_R$  67% higher than in 2010 (Table 5). The  
385 highest daily  $E_R$  attained  $100 \text{ W m}^{-2}$  on 9 July and coincided with the start of a Greenland-

386 wide warm event. On 12 July, nearly the entire ice sheet surface was reported to melt  
387 (Nghiem et al., 2012), followed shortly after by the highest meltwater discharge in 56 years  
388 on 12 July 2012, as ~~inferred can be concluded~~ by the partial destruction of a bridge  
389 ~~constructed over the the 1956~~-Watson river ~~bridge~~ in Kangerlussuaq ~~in 1956. on 12 July 2012.~~  
390 At KAN U, wWell above the long-term ELA ~~at KAN U~~, not only a strongly negative SMB  
391 was recorded in 2012, but it was the only year with a positive annual radiation budget ( $E_R =$   
392  $+4 \text{ W m}^{-2}$ ; Table 5).

393  $E_H$  was largest during 2010 and smallest during 2011 (Table 5), the years of highest and  
394 lowest annual  $T_a$ , respectively (Table 3). Sensible heat transfer toward the ice sheet surface  
395 was also low on average ~~also low~~ in 2012, owing to the cold winter months. The high July  
396 2011  $E_H$  was due to warm air advection that occurred over a cold surface, yielding large near-  
397 surface temperature gradients and ~~thus~~ sensible heat exchange (Fig. 7a). ~~In the~~During summer  
398 ~~of~~ 2013, when ~~the air~~ temperatures remained relatively low, the ice sheet surface exhibited the  
399 lowest sensible heat gain compared to the other melt seasons. In all,  $E_H$  did not contribute to  
400 SEB interannual variability as much as the radiative components.

401 Summer  $E_E$  values are correlated with the atmospheric pressure ( $R = 0.96$ ), which ~~that~~  
402 influences the gradients in near-surface specific humidity and wind speed. ~~In the~~During  
403 summer ~~of~~ 2012, pressure and specific humidity were relatively high (811 hPa and  $3.7 \text{ g kg}^{-1}$ ,  
404 respectively; Table 3), while the wind speed was reduced, thus contributing to the lowest  
405 absolute summer  $E_E$  with the lowest cooling rates due to evaporation/sublimation. The  
406 maximum latent heat loss that year occurred in May. Thereafter, the moisture content in the  
407 near-surface air became relatively large, with  $E_E$  decreasing in absolute value until July.  
408 Summer 2013, was conversely characterized by relatively low pressure and specific humidity  
409 (804 hPa and  $2.8 \text{ g kg}^{-1}$ , respectively) resulting in high evaporation/sublimation rates  
410 especially in June and July (Fig. 7b).

411 Monthly  $E_G$  values were small and displayed small interannual variability, especially in  
412 summer. The summers of 2010 and 2011 exhibited the most positive  $E_G$  as a consequence of  
413 substantial refreezing (Fig. 7c), which influenced ~~impacting the~~ near-surface firn temperature  
414 gradients ~~in the firn~~. ~~The summer average~~Summer  $E_G$  values ~~for in~~ 2009 and 2013 (Table 5)  
415 ~~were was~~ lower due to the moderate melt seasons of smaller duration. Summer  $E_G$  was lower  
416 ~~in~~ summer 2012 due to a warm ice sheet surface conducting heat into the firn and the absence



417 of refreezing.

418 The melt rates in 2009 and 2013 ~~was-were~~ similar. In both years ~~-with-~~ the largest  $E_M$  occurred  
419 ~~ing~~ in July and did not exceed~~ing~~  $30 \text{ W m}^{-2}$  (Fig. 8a).  $E_M$  peaked similarly in 2010 and 2011,  
420 in June reaching about  $20 \text{ W m}^{-2}$  and in July exceeding  $35 \text{ W m}^{-2}$ . May and August 2010  
421 ~~sustained-exhibited~~ significant melt in response to the warm atmospheric conditions (Van As  
422 et al., 2012). Both 2010 and 2012 exhibited significant melt in May ( $10 \text{ W m}^{-2}$ ). During  
423 summer 2012,  $E_M$  far exceeded all other years, with ~~-e.g.-~~ a July value of  $68 \text{ W m}^{-2}$ , leading to  
424 the largest~~st~~ ablation reported in Table 4.

425 ~~There is a large dominance of~~ the radiative fluxes dominate over the interannual variability  
426 of melt at KAN\_U, with the variations in  $E_L^{\text{Net}}$  being most influential over the amount of  
427 available  $E_M$  in the years 2009–2011 and 2013. In 2012, it was the large  $E_S^{\text{Net}}$  that mainly  
428 contributed to the melt anomaly.

### 429 3.4 Melt-albedo feedback

430 Figure 9a, which depicts total monthly surface energy exchanges throughout the study period,  
431 illustrates that  $E_S^{\text{Net}}$  and  $E_L^{\text{Net}}$  dominate the SEB from May to September, while  $E_L^{\text{Net}}$  and  $E_H$   
432 dominate the SEB during the remainder of the year. During the years exclusive of 2012  
433 considered here (2009, 2010, 2011 and 2013), the total summer energy input to the ice sheet  
434 surface was  $620\text{--}650 \text{ MJ m}^{-2}$ . This energy reaches a peak in July. In July 2010, for example,  
435 the total energy input reached  $246 \text{ MJ m}^{-2}$ . By contrast, in 2012, the total summer energy  
436 input exceeded  $770 \text{ MJ m}^{-2}$ , and in July it reached  $304 \text{ MJ m}^{-2}$ . The 2012 total energy used  
437 for melt was  $414 \text{ MJ m}^{-2}$  (65 % higher than in 2010), of which  $183 \text{ MJ m}^{-2}$  was used for melt  
438 in July. Figure 9a shows the total surface energy exchange for each month throughout the  
439 study period. It illustrates that  $E_S^{\text{Net}}$  and  $E_L^{\text{Net}}$  dominate the energy balance during the months  
440 May to September, while  $E_L^{\text{Net}}$  and  $E_H$  govern the SEB during wintertime (Fig. 9a). For the  
441 years 2009–2011 and 2013 the total energy in the summer months was  $1250\text{--}1300 \text{ MJ m}^{-2}$ . In  
442 July, when the energy input is largest, the years 2009 and 2013 exhibited a total amount of  
443 energy of  $464 \text{ MJ m}^{-2}$  while in the years 2010 and 2011 it reached  $500 \text{ MJ m}^{-2}$ . In 2012, the  
444 summer total energy was significantly higher exceeding  $1500 \text{ MJ m}^{-2}$ , while July alone  
445 reached  $608 \text{ MJ m}^{-2}$  with  $183 \text{ MJ m}^{-2}$  invested in melting. The total melt energy in 2012  
446 amounted to  $414 \text{ MJ m}^{-2}$ .



447 Figure 9b illustrates the simulated mass fluxes at the [ice sheet](#) surface (note the different y  
448 scales for positive and negative values). A total of  $40 \text{ kg m}^{-2}$  of mass loss occurs on average  
449 by the sum of sublimation and evaporation during spring and summer. ~~Conversely,~~  
450 ~~Deposition-deposition~~ amounts ~~to~~  $10 \text{ kg m}^{-2}$  each winter season. The total snowfall from  
451 April 2009 until September 2013 amounted  $\sim 1500 \text{ kg m}^{-2}$  (also Table 4). Up to the end of  
452 May 2012, all meltwater had accumulated internally through percolation into the firn, adding  
453 a mass of  $1158 \text{ kg m}^{-2}$  ( $1020 \text{ kg m}^{-2}$  from snowfall and  $138 \text{ kg m}^{-2}$  from rainfall). Due to ice  
454 layer blocking vertical percolation in summer 2012,  $444 \text{ kg m}^{-2}$  ran off, removing  
455 approximately 38% of accumulated mass since April 2009.

456 The total amount of meltwater generated at the [ice sheet](#) surface, ~~equaling equivalent to~~ the  
457 sum of runoff and refreezing ~~minus rainfall~~, amounted ~~1307-1232~~  $\text{kg m}^{-2}$  in 2012. As the  
458 calculated surface ablation was  $860 \text{ kg m}^{-2}$  (Table 4), ~~30-66%~~ (~~372447~~  $\text{kg m}^{-2}$ ) of the  
459 produced meltwater was melted more than once during the ablation season. ~~This suggests that~~  
460 ~~Essentially, 48%~~ ( $416 \text{ kg m}^{-2}$ ) (~~48 %~~ of the total ablation ~~or 34 % of the produced meltwater~~)  
461 was ~~effectively~~ retained ~~in near surface firn layers~~.

462 2010 was the first year on record during which surface ablation exceeded accumulation from  
463 the preceding winter at KAN\_U (Table 4; Van de Wal et al., 2012). Even though atmospheric  
464 temperatures were high and the impact on ablation was large in 2010, the response of the  
465 snow surface was much larger in 2012, when ablation was more than three times larger than  
466 the accumulation. ~~Albedo- In 2012, albedo dropped-decreased~~ to  $\sim 0.7$  ~~already by in~~ mid-June  
467 (Charalampidis and van As, ~~in press~~2015), implying substantial metamorphosis of the snow  
468 surface, while in all other years this ~~value-albedo~~ was reached only in July or August. The  
469 albedo reduced even more on 10 July ( $\sim 0.6$ ), signifying the saturation of the [ice sheet](#) surface  
470 and the exposure of thick firn. Until 6 August, the albedo value corresponded to that of  
471 soaked facies close to the snow/firn line (Cuffey and Paterson, 2010). It should be noted that  
472 snowfall events increased the albedo during several periods in the summer season  
473 (Charalampidis and van As, ~~in press~~2015).

474 ~~To quantify the impact of a relatively dark ice sheet surface on the SEB, T~~ the average annual  
475 cycle in albedo of all years excluding 2012 was used to replace the low 2012 albedo in  
476 ~~dedicated a model-sensitivity analysis run to quantify the impact of a relatively dark ice sheet~~  
477 ~~surface on the SEB~~. Figure 10a shows the albedo anomaly of 2012, which ~~resulted in started~~

478 ~~invoking~~ enhanced ablation in late May/early June (Fig. 10b). At the end of August, the [ice](#)  
479 [sheet](#) surface lowered an additional 0.64 m due to 58% more melt energy compared to a  
480 situation with average albedo. The excess  $E_M$  from the melt-albedo feedback amounted to 152  
481  $\text{MJ m}^{-2}$ , while the excess  $E_S^{\text{Net}}$  supplied was  $213 \text{ MJ m}^{-2}$  (Fig. 10c). The remaining  $E_S^{\text{Net}}$  was  
482 consumed by other fluxes, primarily  $E_H$ . As the total surface ablation of 2012 was 1.78 m of  
483 surface height change (Fig. 2) the remaining 1.14 m was primarily due to the warm  
484 atmospheric conditions and similar to 2010 (1.21 m). This [sensitivity analysis](#) implies that the  
485 location would have experienced a negative SMB in 2012 even without the melt-albedo  
486 feedback.

487

## 488 **4 Discussion**

### 489 **4.1 Uncertainties**

490 Model performance is limited by the accuracy of the instruments of KAN\_U as given in Table  
491 1. The radiometer uncertainties are the largest, based on what is reported by the manufacturer  
492 (10% for daily totals, although this is likely to be an overestimate (Van den Broeke et al.,  
493 2004)). Nevertheless, the accurate simulation of surface temperature and snow ablation rates  
494 (Fig. 2) throughout the period of observations builds confidence in both the measurements  
495 and the model.

496 The model exhibits considerable sensitivity to the subsurface calculations, suggesting  
497 importance of pore volume and firn temperature, and how much more complicated SEB  
498 calculations are in the lower accumulation area than for bare ice in the ablation area. The  
499 model is able to capture the seasonal variations of temperature in the firn and calculated  
500 temperatures are commonly within  $3.6 \text{ }^\circ\text{C}$  of those measured with an average of  $-0.3 \text{ }^\circ\text{C}$  (Fig.  
501 11a). The shallow percolation of a wetting front in the firn is estimated at depths of 1–3 m in  
502 the years 2009 and 2013 (Fig. 11b), while in the years of larger melt, pore volume until 10 m  
503 depth is filled, possibly overestimating the percolation depth given the relative temperature  
504 buildup in the simulated firn below roughly 5 m depth (Fig. 11a; [Charalampidis et al., under](#)  
505 [review](#)). In particular for 2012, available simulated pore volume at ~6 m is significantly  
506 affected by meltwater that percolates below the formed thick ice layer, which may indicate  
507 that the runoff threshold of a 6 m ice layer is an overestimate, highlighting the need for a

508 better runoff criterion. Further investigation on this criterion and inclusion of water content  
509 held in the firn by capillary forces, saturation of the surface and proximity of impermeable ice  
510 to the surface is necessary.

511 The fact that the subsurface calculations are initialized in 2009 by use of vertically shifted firn  
512 densities from a 2012 core does not influence the calculation of the surface energy fluxes and  
513 thus the outcome of this paper. Importantly, the timing that simulated runoff occurred in July  
514 2012 is in agreement with satellite observations due to the runoff criterion, thereby providing  
515 confidence in realistic calculation of  $E_G$ .

516 Although the subsurface calculations are on a vertical grid of 10 cm (see also 2.3), there is  
517 loss of detail in the density profile with time due to the interpolation scheme that shifts the  
518 column vertically when it needs to account for surface height variations (Fig. 11c). Increased  
519 spatial resolution requires a finer temporal resolution to avoid model instability. Since this  
520 would also increase calculation time severely, while the calculated SEB would be unaffected,  
521 we accepted the loss of detail in density in this study. Nevertheless, during each melt season  
522 when refreezing is important to be accounted for, no loss of detail is expected near the surface  
523 since the column is shifted almost continuously upward.

524 Rainfall is known to occur during summer on the higher elevations of the ice sheet. The exact  
525 amount is unknown as in situ measurements for precipitation are rare and difficult. Therefore,  
526 the rainfall calculated by our model should be considered a first-order estimate. Nevertheless,  
527 the amount of rain is expected to be small and its effect on the SEB is negligible, as shown by  
528 the model results.

529 It is possible that other factors than heat-induced snow metamorphism and the presence of  
530 surface water contributed to the 2012 albedo anomaly. Such could be aerosol particles or  
531 impurities at the snow surface, effectively reducing its albedo (Doherty et al., 2013). Also, in  
532 cases of extreme melt, microbial activity can develop at the [ice sheet](#) surface with the  
533 subsequent production of a dark-colored pigment (Benning et al., 2014).

## 534 **4.2 Long-term perspective in temperature and albedo**

535 ~~The regional barometric pressure is linked to the NAO with KAN\_U measurements exhibiting~~  
536 ~~a negative correlation ( $R = -0.72$  for monthly averages) with the NAO index. The correlation~~

537 ~~between the NAO index and pressure in west Greenland implies that the variability of the~~  
538 ~~regional climate is partly controlled by the North Atlantic climate (Figs. 12a,b). For instance,~~  
539 ~~warm summers on the ice sheet coincide with extended periods of negative NAO index.~~ The  
540 Kangerlussuaq airport temperature record since 1976 was used to provide a temporal  
541 perspective to the KAN\_U temperature in recent years (Fig. 12c). The standard deviations  
542 reveal variability during the winter period of more than 10 °C while for the months of July  
543 and August standard deviations are ~2.0 °C. The temperature measurements reveal that the  
544 region has been warming on average starting in 1996 (not shown). Figure 12d illustrates this  
545 for 2000–2013; e.g. the summers (JJA) were 1.2 °C warmer than in the reference period  
546 1976–1999. The warm 2010 and 2012 summer have an anomaly value of +1.9 °C and +1.8  
547 °C, respectively. The high temperatures in recent years are most apparent for June when in 10  
548 out of 14 years the 1976–1999 standard deviation is exceeded. A further increase of the  
549 regional temperatures, as anticipated by climate models, will likely further increase the  
550 frequency of large melt events and the extent of each melt season, leading to conditions  
551 similar to or more extreme than in 2012 (McGrath et al., 2013).

552 The MOD10A1 time series from the years 2000–2013 shows an albedo decrease of 0.05–0.10  
553 during the 14 years of measurements in response to the increased temperatures (Fig. 13). In  
554 particular, May albedo reached record low values in 2010 and 2012. July albedo is  
555 considerably lower in the years 2007–2013 than it was in the first half of the record. The  
556 exceptional surface conditions in July 2012 were also captured by MODIS with the lowest  
557 monthly albedo (~0.6) of the time series. The albedo in August is generally higher than in  
558 July due to snowfall, but the values remain sufficiently low to enhance melt. We note that part  
559 of the MODIS based albedo decrease could be the result of the declining instrument  
560 sensitivity of the Terra MODIS sensor (Wang et al. 2012; Lyapustin et al. 2014) though  
561 updated (through 2014) comparisons between MOD10A1 and ground observations from GC-  
562 Net data (Box et al. 2012; not shown) do not indicate an obvious nor statistically significant  
563 difference.

564 Increased meltwater infiltration into the firn during events of increased melt has led to the  
565 formation of thick, near-surface ice lenses between 2 to 7 m, judging from the 2012 firn core.  
566 This contrasts the aquifers (i.e. liquid water storage) that are observed in the firn in southeast  
567 Greenland (Forster et al., 2013; Koenig et al., 2014; Kuipers Munneke et al., 2014). The  
568 southwest~~ern~~ ice sheet receives about one third of the annual precipitation amount in the

569 southeast (Ettema et al., 2009), resulting in differences in thermal insulation of the infiltrated  
570 water and available pore volume. Persistent shallow refreezing on an interannual scale has led  
571 to the formation of thick impermeable ice enabling runoff in 2012 (Machguth et al., under  
572 review).

573 The DMI measurements indicate that 2009 is representative of the reference period 1976–  
574 1999 (Fig. 11c; Van As et al., 2012). ~~In summer~~With respect to summer 2009, 2010–the  
575 radiation budget in summer 2010 was increased due to ~~reduced-lower~~  $E_L^{\text{Net}}$  ~~by~~  $10 \text{ W m}^{-2}$   
576 (Table 5; Sect. 3.3). ~~The concurrent increase in melt was~~  $13 \text{ W m}^{-2}$ . In summer 2012,  $E_L^{\text{Net}}$   
577 was the same, while  $E_S^{\text{Net}}$  was ~~17~~  $17 \text{ W m}^{-2}$ -larger than in 2010. ~~, approximately 70% Most~~ of  
578 ~~which this~~  $E_S^{\text{Net}}$  excess was consumed by melting (~~12~~  $12 \text{ W m}^{-2}$ ; Sect. 3.4). The melt-albedo  
579 feedback (Box et al., 2012) will contribute to the rise of the ELA in a warming climate  
580 (Fettweis, 2007; Van de Wal et al., 2012), and might transform the lower accumulation area  
581 into superimposed ice if warming prevails. We have shown that the melt-albedo feedback  
582 makes that warm summers can have great impact on melt and runoff in the lower  
583 accumulation area. Our results suggest that if warm atmospheric conditions persist in the  
584 future, the additional input of solar radiation at the ice sheet surface will be of higher  
585 importance to surface changes than atmospheric warming.

586

## 587 **5 Conclusions**

588 We used five years of automatic weather station measurements to characterize the prevailing  
589 meteorology and surface energy fluxes at a location in the lower accumulation area of the  
590 southwest Greenland ice sheet. The analysis showed large control of the radiative components  
591 over the interannual variability, and mostly from net longwave radiation. The main  
592 contributor to melt is absorbed solar ~~radiation~~radiation. ~~In n, but for~~ all but one year of  
593 observations, ~~however, this solar radiation~~ did not ~~induce-control~~ surface mass balance  
594 variability. This was not the case during the 2012 melt season, when the area attained  
595 unusually low albedo values ( $<0.7$ ) owing to large melt and the subsequent exposure of water-  
596 saturated, high-density firn. The consequent~~ial~~ enhanced solar absorption along with warm  
597 atmospheric conditions resulted in intensified melt during the ~~strongest-most~~ negative surface  
598 mass budget year since 1994, and presumably since at least 1976 given the Kangerlussuaq  
599 temperature record. A sensitivity test with our energy balance model indicates that the melt-

600 | albedo feedback contributed an additional 58\_% (152 MJ m<sup>-2</sup>) to melt energy in 2012, though  
601 | increased atmospheric temperatures alone would have yielded a negative surface mass budget  
602 | as well.

603 | Percolation of meltwater within snow and firn is generally considered to refreeze in firn at  
604 | 1840 m a.s.l. on the ice sheet, which prevents runoff and therefore limits Greenland's  
605 | contribution to sea level rise. This ~~concept is applicable applies~~ to all ~~the~~ higher elevation  
606 | regions of the ice sheet ~~where there is that experience~~ moderate melt and ~~where~~ deep  
607 | percolation is possible. However, the lower accumulation area of the southwestern ice sheet  
608 | showed high sensitivity to the warm atmosphere in 2012, primarily ~~due to because of~~ the  
609 | relatively low precipitation in the region, which prevents the timely replenishment of  
610 | saturated enables the immediate loss of pore volume in the near surface upper meters of firn  
611 | under extreme melting conditions. Water retained in the firn can lead to substantial density  
612 | increase due to refreezing, which in warm years not only may function as a mechanism to  
613 | block percolation, but also lowers the surface albedo and enhances melt, accelerating the  
614 | transformation of ~~the a~~ lower accumulation area underlain by firn into an ablation-dominated  
615 | region area underlain by superimposed ice. This highlights the importance of accurately  
616 | modelling ~~of~~ percolation and refreezing within the firn, in order to ~~best be able to~~ estimate the  
617 | sea level rise contribution associated with ~~from the~~ Greenland ice sheet ~~to sea level~~  
618 | rise meltwater production.

619 |

## 620 | **Acknowledgements**

621 | We are grateful to Xavier Fettweis and an anonymous reviewer for constructive comments.  
622 | We also thank Andreas Mikkelsen for snow density measurements, and Robert Fausto,  
623 | Filippo Calì Quaglia and Daniel Binder for valuable discussions. The KAN U weather station  
624 | was funded by the nuclear waste management organizations in Sweden (Svensk  
625 | Kärnbränslehantering AB), Finland (Posiva Oy) and Canada (NWMO) through the Greenland  
626 | Analogue Project (GAP Sub-Project A). It is operated by the Geological Survey of Denmark  
627 | and Greenland (GEUS) with 2009–2012 logistical, technical and manpower support from  
628 | Aberystwyth University funded through the UK Natural Environmental Research Council  
629 | (NERC grant NE/G005796/1), a Royal Geographical Society (RGS) Gilchrist Fieldwork  
630 | Award, and an Aberystwyth University doctoral scholarship. Technical and salary support

631 were received from the Programme for Monitoring of the Greenland Ice Sheet (PROMICE),  
632 launched and funded by the Danish Energy Agency (Energistyrelsen) under the Danish  
633 Ministry of Energy, Utilities and Climate, and within the Danish Cooperation for  
634 Environment in the Arctic (DANCEA). We further acknowledge support from the  
635 Netherlands Polar Programme of the Netherlands Organization for Scientific Research  
636 (NWO). This is a PROMICE publication and contribution number 52 of the Nordic Centre of  
637 Excellence SVALI, “Stability and Variations of Arctic Land Ice”, funded by the Nordic Top-  
638 level Research Initiative (TRI).We thank Andreas Mikkelsen for collection of snow densities,  
639 Alun Hubbard and Samuel Doyle for retrieval of KAN\_U weather station measurements and  
640 Robert Fausto, Filippo Cali Quaglia and Daniel Binder for valuable discussions. The KAN  
641 weather stations are financed by the Greenland Analogue Project (GAP) and operated by the  
642 Geological Survey of Denmark and Greenland (GEUS). We also acknowledge support from  
643 the Netherlands Polar Programme of the Netherlands Organization for Scientific Research,  
644 section Earth and Life Sciences (NWO/ALW). This is a publication in the framework of the  
645 Programme for Monitoring of the Greenland Ice Sheet (PROMICE) and contribution number  
646 52 of the Nordic Centre of Excellence SVALI, ‘Stability and Variations of Arctic Land Ice’,  
647 funded by the Nordic Top-level Research Initiative (TRI).

648



649 **References**

650 [Ahlstrøm, A. P. and the PROMICE project team: A new programme for monitoring the mass](#)  
651 [loss of the Greenland ice sheet, Geol. Surv. Denmark Greenland Bull., 15, 61–64,](#)  
652 [2008.](#) ~~Ahlstrøm, A. P., van As, D., Citterio, M., Andersen, S. B., Nick, F. M., Gravesen, P.,~~  
653 ~~Edelvang, K., Fausto, R. S., Andersen, M. L., Kristensen, S. S., Christensen, E. L., Boncori, J.~~  
654 ~~P. M., Dall, J., Forsberg, R., Stenseng, L., Hanson, S., and Petersen, D.: Final report for the~~  
655 ~~establishment phase of the Programme for Monitoring of the Greenland Ice Sheet, Tech. rep.,~~  
656 ~~Danmarks og Grønlands Geologiske Undersøgelse Rapport 2011/18, 2011.~~

657 Andreas, E. L.: A theory for the scalar roughness and the scalar transfer coefficients over  
658 snow and sea ice. *Bound.-Lay. Meteorol.*, 38(1–2), 159–184, doi:10.1007/BF00121562,  
659 1987.

660 Ambach, W.: The influence of cloudiness on the net radiation balance of a snow surface with  
661 high albedo. *J. Glaciol.*, 13, 73–84, 1974.

662 Bamber, J. L., Griggs, J. A., Hurkmans, R. T. W. L., Dowdeswell, J. A., Gogineni, S. P.,  
663 Howat, I., Mouginot, J., Paden, J., Palmer, S., Rignot, E., and Steinhage, D.: A new bed  
664 elevation dataset for Greenland, [The CryosphereCryosph.](#), 7, 499–510, doi:10.5194/tc-7-499-  
665 2013, 2013.

666 Bennartz, R., Shupe, M. D., Turner, D. D., Walden, V. P., Steffen, K., Cox, C. J., Kulie, M.  
667 S., Miller, N. B., and Pettersen, C.: July 2012 Greenland melt extent enhanced by low-level  
668 liquid clouds, *Nature*, 496, 83–86, doi:10.1038/Nature12002, 2013.

669 Benning, L. G., Anesio, A. M., Lutz, S., and Tranter, M.: Biological impact on Greenland's  
670 albedo, [Nature-Nat. GeoscienceGeosci.](#), 7, 691, doi:10.1038/ngeo2260, 2014.

671 Bøggild, C. E., Brandt, R. E., Brown, K. J., and Warren, S. G.: The ablation zone in northeast  
672 Greenland: Ice types, albedos, and impurities, *J. Glaciol.*, 56, 101–113,  
673 doi:10.3189/002214310791190776, 2010.

674 Box, J. E., Fettweis, X., Stroeve, J. C., Tedesco, M., Hall D. K., and Steffen, K.: Greenland  
675 ice sheet albedo feedback: thermodynamics and atmospheric drivers, [The](#)  
676 [CryosphereCryosph.](#), 6, 821–839, doi:10.5194/tc-6-821-2012, 2012.

677 Cappelen, J.: Weather Observations from Greenland 1958–2012. Technical Report 13–11,



678 Danish Meteorological Institute, Ministry of Climate and Energy, 2013.

679 Charalampidis, C. and van As, D.: Observed melt-season snowpack evolution on the  
680 Greenland ice sheet, *Geol. Surv. Denmark Greenland Bull.*, [33, 65–68, 2015](#).in press.

681 [Charalampidis, C., van As, D., Colgan, W. T., Fausto, R. S., MacFerrin M., and Machguth H.:](#)  
682 [Thermal tracing of retained meltwater in the lower accumulation area of the southwestern](#)  
683 [Greenland ice sheet, \*Ann. Glaciol.\*, under review.](#)

684 [Citterio, M., van As, D., Ahlstrøm, A. P., Andersen, M. L., Andersen, S. B., Box, J. E.,](#)  
685 [Charalampidis, C., Colgan, W. T., Fausto, R. S., Nielsen, S., and Veicherts, M.: Automatic](#)  
686 [weather stations for basic and applied glaciological research, \*Geol. Surv. Denmark Greenland\*](#)  
687 [Bull.](#), [33, 69–72, 2015.](#)

688 Cuffey, K. M., and Paterson, W.: *The physics of glaciers*, Elsevier, 693 pp., 2010.

689 Doherty, S. J., Grenfell, T. C., Forsström, S., Hegg, D. L., Brandt, R. E., and Warren, S. G.:  
690 Observed vertical redistribution of black carbon and other insoluble light-absorbing particles  
691 in melting snow, *J. Geophys. Res. Atmos.*, 118, 5553–5569, doi:10.1002/jgrd.50235, 2013.

692 Enderlin, E. M., Howat, I. M., Jeong, S., Noh, M.-J., van Angelen, J. H., and van den Broeke,  
693 M. R.: An improved mass budget for the Greenland ice sheet, *Geophys. Res. Lett.*, 41, 866–  
694 872, doi:10.1002/2013GL059010, 2014.

695 Ettema, J., van den Broeke, M. R., van Meijgaard, E., van de Berg, W. J., Bamber, J. L., Box,  
696 J. E., and Bales, R. C.: Higher surface mass balance of the Greenland ice sheet revealed by  
697 high-resolution climate modeling, *Geophys. Res. Lett.*, 36, L12501,  
698 doi:10.1029/2009GL038110, 2009.

699 Ettema, J., van den Broeke, M. R., van Meijgaard, E., and van de Berg, W. J.: Climate of the  
700 Greenland ice sheet using a high-resolution climate model–Part 2: Near-surface climate and  
701 energy balance, [The CryosphereCryosph.](#), 4(4), 529–544, doi:10.5194/tc-4-529-2010, 2010.

702 Fettweis, X.: Reconstruction of the 1979–2006 Greenland ice sheet surface mass balance  
703 using the regional climate model MAR, [The CryosphereCryosph.](#), 1, 21–40, doi:10.5194/tc-  
704 1-21-2007, 2007.

705 Forster, R. R., Box, J. E., van den Broeke, M. R., Miège, C., Burgess, E. W., van Angelen, J.  
706 H., Lenaerts, J. T. M., Koenig, L. S., Paden, J., Lewis, C., Gogineni, S. P., Leuschen C., and  
707 McConnell, J. R.: Extensive liquid melt water storage in firn within the Greenland ice sheet,  
708 *Nat. Geosci.*, doi: 10.1038/NGEO2043, 2013.

709 Greuell, W.: Melt water accumulation on the surface of the Greenland ice sheet: Effect on  
710 albedo and mass balance, *Geografiska Annaler: Series A, Phys. Geogr.*, 82(4):489–498, doi:  
711 10.1111/j.0435-3676.2000.00136.x, 2000.

712 Greuell, W., Denby, B., van de Wal, R. S. W., and Oerlemans, J.: Correspondance. 10 years  
713 of mass- balance measurements along a transect near Kangerlussuaq, central west Greenland,  
714 *J. Glaciol.*, 47(156):157–158, 2001.

715 Hanna, E., Fettweis, X., Mernild, S. H., Cappelen, J., Ribergaard, M. H., Shuman, C. A.,  
716 Steffen, K., Wood, L., and Mote, T. L.: Atmospheric and oceanic climate forcing of the  
717 exceptional Greenland ice sheet surface melt in summer 2012, *Int. J. Climatol.*, doi:  
718 10.1002/joc.3743, 2014.

719 Harper, J., Humphrey, N., Pfeffer, W. T., Brown, J., and Fettweis, X.: Greenland ice-sheet  
720 contribution to sea-level rise buffered by melt water storage in firn, *Nature*, 491, 240–243,  
721 doi:10.1038/nature11566, 2012.

722 Henneken, E. A. C., Bink, N. J., Vugts, H. F., Cannemeijer, F., Meesters, A. G. C. A.: A case  
723 study of the daily energy balance near the equilibrium line on the Greenland ice sheet, *Global*  
724 *Planet. Change*, 9, 69–78, doi:10.1016/0921-8181(94)90008-6, 1994.

725 Huybrechts, P., and de Wolde, J.: The dynamic response of the Greenland and Antarctic ice  
726 sheets to multiple-century climatic warming. *J. Climate*, 12, 2169–2188, doi:10.1175/1520-  
727 0442(1999)012<2169:TDROTG>2.0.CO;2, 1999.

728 Huybrechts, P., Goelzer, H., Janssens, I., Driesschaert, E., Fichet, T., Goosse, H., and  
729 Loutre, M. F.: Response of the Greenland and Antarctic Ice Sheets to Multi-Millennial  
730 Greenhouse Warming in the Earth System Model of Intermediate Complexity LOVECLIM,  
731 *Surv. Geophys.*, 32, 397–416, doi:10.1007/s10712-011-9131-5, 2011.

732 Illangasekare, T. H., Walter, R. J., Meier, Jr., M. F., and Pfeffer, W. T.: Modeling of melt

733 water infiltration in subfreezing snow, *Water Resources Res.*, 26–5, 1001–1012,  
734 doi:10.1029/WR026i005p01001, 1990.

735 Koenig, L. S., Miège, C., Forster, R. R., and Brucker, L.: Initial in situ measurements of  
736 perennial melt water storage in the Greenland firn aquifer, *Geophys. Res. Lett.*,  
737 doi:10.1002/2013GL058083, 2013.

738 Kuipers Munneke, P., Ligtenberg, S. R. M., van den Broeke, M. R., van Angelen, J. H., and  
739 Forster, R. R.: Explaining the presence of perennial liquid water bodies in the firn of the  
740 Greenland Ice Sheet, *Geophys. Res. Lett.*, 41, doi:10.1002/2013GL058389, 2014.

741 Lenaerts, J. T. M., Smeets, C. J. P. P., Nishimura, K., Eijkelboom, M., Boot, W., van den  
742 Broeke, M. R., and van de Berg, W.J.: Drifting snow measurements on the Greenland Ice  
743 Sheet and their application for model evaluation, ~~The Cryosphere~~[Cryosph.](#), 8, 801–814,  
744 doi:10.5194/tc-8-801-2014, 2014.

745 [Lyapustin, A., Wang, Y., Xiong, X., Meister, G., Platnick, S., Levy, R., Franz, B., Korkin, S.,](#)  
746 [Hilker, T., Tucker, J., Hall, F., Sellers, P., Wu, A., and Angal, A.: Scientific impact of](#)  
747 [MODIS C5 calibration degradation and C6+ improvements, \*Atmos. Meas. Tech.\*, 7, 4353–](#)  
748 [4365, doi:10.5194/amt-7-4353-2014, 2014.](#)

749 Machguth, H., MacFerrin, M., van As, D., Box, J. E., Charalampidis, C., Colgan, W. T.,  
750 Fausto, R. S., Meijer, H. A. J., Mosley-Thompson, E. and van de Wal, R. S. W.: [Greenland](#)  
751 [meltwater storage in firn limited by near-surface ice formation](#)~~Successive and intense melt~~  
752 ~~rapidly decreases Greenland meltwater retention in firn~~, *Nat. Clim. Change*, under review.

753 MacWhorter, M. A., and Weller, R. A.: Error in measurements of incoming shortwave  
754 radiation made from ships and buoys, *J. Atmos. Oceanic Technol.*, 8:, 108–117,  
755 doi:10.1175/1520-0426(1991)008<0108:EIMOIS>2.0.CO;2, 1991.

756 McGrath, D., Colgan, W., Bayou, N., Muto, A., and Steffen, K.: Recent warming at Summit,  
757 Greenland: Global context and implications, *Geophys. Res. Lett.*, 40, doi:10.1002/grl.50456,  
758 2013.

759 Nghiem, S. V., Hall, D. K., Mote, T. L., Tedesco, M., Albert, M. R., Keegan, K., Shuman, C.  
760 A., DiGirolamo, N. E., and Neumann, G.: The extreme melt across the Greenland ice sheet in

761 2012, *Geophys. Res. Lett.*, 39(20), L20502, doi:10.1029/2012GL053611, 2012.

762 Shepherd, A., Ivins, E. R., A, G., Barletta, V. R., Bentley, M. J., Bettadpur, S., Briggs, K. H.,  
763 Bromwich, D. H., Forsberg, R., Galin, N., Horwath, M., Jacobs, S., Joughin, I., King, M. A.,  
764 Lenaerts, J. T. M., Li, J., Ligtenberg, S. R. M., Luckman, A., Luthcke, S. B., McMillan, M.,  
765 Meister, R., Milne, G., Mouginot, J., Muir, A., Nicolas, J. P., Paden, J., Payne, A. J.,  
766 Pritchard, H., Rignot, E., Rott, H., Sandberg Sørensen, L., Scambos, T. A., Scheuchl, B.,  
767 Schrama, E. J. O., Smith, B., Sundal, A. V., van Angelen, J. H., van de Berg, W. J., van den  
768 Broeke, M. R., Vaughan, D. G., Velicogna, I., Wahr, J., Whitehouse, P. L., Wingham, D. J.,  
769 Yi, D., Young, D., and Zwally, H. J.: A reconciled estimate of ice-sheet mass balance,  
770 *Science*, 338 (6111), 1183–1189, doi:10.1126/science.1228102, 30 November 2012.

771 Smeets, C. J. P. P. and van den Broeke, M. R.: Temporal and spatial variations of the  
772 aerodynamic roughness length in the ablation zone of the Greenland ice sheet, *Bound.-Lay.*  
773 | *Meteorol.*, 128(3):, 315–338, ~~ISSN 0006-8314~~, doi: 10.1007/s10546-008-9291-0, 2008.

774 Solomon, S., Qin, D., Manning, M., Chen, Z., Marquis, M., Averyt, K. B., Tignor, M., and  
775 Miller, H.L. (eds.): IPCC. *Climate Change 2007: The Physical Science Basis*. Contribution of  
776 Working Group I to the Fourth Assessment Report of the Intergovernmental Panel on Climate  
777 Change Cambridge University Press, Cambridge, United Kingdom and New York, NY, USA,  
778 996 pp, 2007.

779 Sturm, M., Holmgren, J., Köning, M., and Morris, K.: The thermal conductivity of seasonal  
780 | snow, *J. Glaciol.*, 43 (143):, 26–41, 1997.

781 Tedesco, M., Fettweis, X., van den Broeke, M. R., van de Wal, R. S. W., Smeets, C. J. P. P.,  
782 van de Berg, W. J., Serreze, M. C., and Box, J. E.: The role of albedo and accumulation in the  
783 | 2010 melting record in Greenland, *Environ. Res. Lett.*, 6(1):, 014005, doi:10.1088/1748-  
784 9326/6/1/014005, 2011.

785 Tedesco, M., Fettweis, X., Mote, T., Wahr, J., Box, J. E., Alexander, P., and Wouters, B.:  
786 Evidence and analysis of 2012 Greenland records from spaceborne observations, a regional  
787 | climate model and reanalysis data, ~~The Cryosphere~~*Cryosph.*, 7, 615–630, doi:-10.5194/tc-7-  
788 615-2013, 2013.

789 Van Angelen, J. H., van den Broeke, M. R., and van de Berg, W. J.: Momentum budget of the

790 atmospheric boundary layer over the Greenland ice sheet and its surrounding seas, *J.*  
791 *Geophys. Res.- Atmos.*, 116, D10101, doi:10.1029/2010JD015485, 2011.

792 Van Angelen, J. H., Lenaerts, J. T. M., van den Broeke, M. R., Fettweis, X., and Meijgaard,  
793 E.: Rapid loss of firn pore space accelerates 21st century Greenland mass loss, *Geoph. Res.*  
794 *Let.*, 40, 2109–2113, doi:-10.1002/grl.50490, 2013.

795 Van As, D., van den Broeke, M. R., Reijmer, C. H., and van de Wal, R. S. W.: The summer  
796 surface energy balance of the high Antarctic plateau, *Bound.-Lay. Meteorol.*, 115(2), 289–  
797 317, doi:-10.1007/s10546-004-4631-1, 2005.

798 Van As, D.: Warming, glacier melt and surface energy budget from weather station  
799 observations in the Melville Bay region of northwest Greenland, *J. Glaciol.*, 57, 208–220,  
800 doi:10.3189/002214311796405898, 2011.

801 Van As, D., Hubbard, A. L., Hasholt, B., Mikkelsen, A. B., van den Broeke, M. R., and  
802 Fausto, R. S.: Large surface melt water discharge from the Kangerlussuaq sector of the  
803 Greenland ice sheet during the record-warm year 2010 explained by detailed energy balance  
804 observations, [The Cryosphere](#), 6(1), 199–209, doi:-10.5194/tc-6-199-2012, 2012.

805 Van As, D., Fausto, R. S., Colgan, W. T., Box, J. E., and the PROMICE project team:  
806 Darkening of the Greenland ice sheet due to the melt-albedo feedback observed at the  
807 PROMICE weather stations, *Geol. Surv. Denmark Greenland Bull.*, 28, 69–72, 2013.

808 Van As, D., Fausto, R. S., Steffen K. and the PROMICE project team: Katabatic winds and  
809 piteraq storms: observations from the Greenland ice sheet, *Geol. Surv. Denmark Greenland*  
810 *Bull.*, 31, 83–86, 2014.

811 Van de Wal, R. S. W., Bintanja, R., Boot, W., van den Broeke, M. R., Conrads, L. A.,  
812 Duynkerke, P. G., Fortuin, P., Henneken, E. A. C., Knap, W. H. L., Portanger, M., Vugts, H.  
813 F. and Oerlemans, J.: Mass balance measurements in the Søndre Strømfjord area in the period  
814 1990-1994, *Z. Gletscherkd. Glazialgeol.*, 31, Part 1, 57–63, 1995.

815 Van de Wal, R. S. W., Greuell, W., van den Broeke, M. R., Reijmer, C. H., and Oerlemans, J.:  
816 Surface mass-balance observations and automatic weather station data along a transect near

817 | Kangerlussuaq, Greenland, *Ann. Glaciol.*, 42(1), [311–316](#)(6),  
818 | doi:10.3189/172756405781812529, 2005.

819 | Van de Wal, R. S. W., Boot, W., Smeets, C. J. P. P., Snellen, H., van den Broeke, M. R., and  
820 | Oerlemans, J.: Twenty-one years of mass balance observations along the K-transect, west  
821 | Greenland, *Earth Syst. Sci. Data*, 4(1), [31–35](#), doi:10.5194/essd-4-31-2012, 2012.

822 | Van den Broeke, M. R., van As, D., Reijmer, C. and van de Wal, R.: Assessing and  
823 | Improving the Quality of Unattended Radiation Observations in Antarctica, *J. Atmos.*  
824 | *Oceanic Technol.*, 21, 1417–1431, doi:10.1175/1520-  
825 | 0426(2004)021<1417:AAITQO>2.0.CO;2, 2004.

826 | Van den Broeke, M. R., Smeets, C. J. P. P., Ettema, J., and Munneke, P. K.: Surface radiation  
827 | balance in the ablation zone of the west Greenland ice sheet, *J. Geophys. Res.- Atmos.*,  
828 | 113(D13), [n/a–n/a](#), ISSN 2156-2202, doi: 10.1029/2007JD009283, 2008a.

829 | Van den Broeke, M. R., Smeets, C. J. P. P., Ettema, J., van der Veen, C., van de Wal, R. S.  
830 | W., and Oerlemans, J.: Partitioning of melt energy and melt water fluxes in the ablation zone  
831 | of the west Greenland ice sheet. [The CryosphereCryosph.](#), 2(2), [179–189](#), doi:-10.5194/tc-2-  
832 | 179-2008, 2008b.

833 | Van den Broeke, M. R., Smeets, C. J. P. P., and Ettema, J.: Surface layer climate and  
834 | turbulent exchange in the ablation zone of the west Greenland ice sheet, *Int. J. Climatol.*,  
835 | 29(15), [2309–2323](#), doi:-10.1002/joc.1815, 2009.

836 | Van den Broeke, M. R., Smeets, C. J. P. P., and van de Wal, R. S. W.: The seasonal cycle and  
837 | interannual variability of surface energy balance and melt in the ablation zone of the west  
838 | Greenland ice sheet. [The CryosphereCryosph.](#), 5(2), [377–390](#), doi:-10.5194/tc-5-377-2011,  
839 | 2011.

840 | Vaughan, D. G., Comiso, J. C., Allison, I., Carrasco, J., Kaser, G., Kwok, R., Mote, P.,  
841 | Murray, T., Paul, F., Ren, J., Rignot, E., Solomina, O., Steffen, K. and Zhang, T.:  
842 | Observations: Cryosphere. In: *Climate Change 2013: The Physical Science Basis.*  
843 | Contribution of Working Group I to the Fifth Assessment Report of the Intergovernmental  
844 | Panel on Climate Change [Stocker, T. F., Qin, D., Plattner, G.-K., Tignor, M., Allen, S. K.,  
845 | Boschung, J., Nauels, A., Xia, Y., Bex, V., and Midgley, P. M. (eds.)], Cambridge University

846 | Press, Cambridge, United Kingdom and New York, NY, USA, 2013.

847 | [Vernon, C. L., Bamber, J. L., Box, J. E., van den Broeke, M. R., Fettweis, X., Hanna, E., and](#)  
848 | [Huybrechts, P.: Surface mass balance model intercomparison for the Greenland ice sheet.](#)  
849 | [Cryosph., 7, 599–614, doi:10.5194/tc-7-599-2013, 2013.](#)

850 | [Wang, D. D., Morton, D., Masek, J., Wu, A. A., Nagol, J., Xiong, X., Levy, R., Vermote, E.,](#)  
851 | [and Wolfe, R.: Impact of sensor degradation on the MODIS NDVI time series, Remote Sens.](#)  
852 | [Environ., 119, 55–61, doi:10.1016/j.rse.2011.12.001, 2012.](#)

853 | Wientjes, I. G. M., and Oerlemans, J.: An explanation for the dark region in the western melt  
854 | zone of the Greenland ice sheet, ~~The Cryosphere~~[Cryosph.](#), 4, 261–268, doi:10.5194/tc-4-261-  
855 | 2010, 2010.

856 | Yen, Y. C.: Review of thermal properties of snow, ice and sea ice. Technical report, USA  
857 | Cold Regions Research and Engineering Laboratory, CRREL Report, 81–10, 1981.

858

859 | Table 1. Sensors and their published accuracies ~~according to the issued manuals~~.

parameter	sensor	accuracy
air pressure	Campbell CS100	2 hPa at -40 °C to 60 °C
aspirated air temperature	Rotronic MP100H aspirated (Pt100)	0.03 °C at 0 °C
relative humidity	Rotronic MP100H aspirated (HygroClip R3)	1.5% at 23 °C
shortwave radiation (incoming and reflected)	Kipp & Zonen CNR4 (Pyranometer)	10% for daily totals
longwave radiation (incoming and emitted)	Kipp & Zonen CNR4 (Pyrgeometer)	10% for daily totals
wind speed and direction	Young 05103-5	0.3 m s <sup>-1</sup> ; 3°
surface height	Campbell SR50A	10 <sup>-2</sup> m or 0.4%

860



861 Table 2. Linear regression parameters for hourly values of KAN\_U and S10 AWSs: Slope ( $\chi$ ),  
 862 intercept ( $\psi$ ), correlation coefficients (R) and rRoot-mMean-sSquared deviations (RMSD).

S10-KAN_U	$\chi$	$\psi$	R	RMSD
$E_S^{\downarrow*}$	1.010	-	0.99	37.25 ( $\text{W m}^{-2}$ )
$E_S^{\uparrow*}$	0.987	-	0.99	24.71 ( $\text{W m}^{-2}$ )
$E_L^{\downarrow}$	1.003	-6.06	0.99	8.92 ( $\text{W m}^{-2}$ )
$E_L^{\uparrow}$	0.990	-0.25	1.00	3.62 ( $\text{W m}^{-2}$ )
$T_a$	0.995	-0.25	1.00	0.50 ( $^{\circ}\text{C}$ )
ambient air pressure	0.990	7.77	1.00	0.45 (hPa)
relative humidity	0.899	10.31	0.91	3.78 (%)
wind speed*	0.928	-	0.99	0.66 ( $\text{m s}^{-1}$ )
$\alpha_{2010}^{**}$	-	-	0.93	0.032 (-)
$\alpha_{2011}^{**}$	-	-	0.94	0.028 (-)
$\alpha_{2012}^{**}$	-	-	0.91	0.066 (-)

\* regression line forced through zero

\*\* 24-hour running averages for the months May until September

863

864 Table 3. Annual and summer (June-July-August) average meteorological parameters at  
 865 KAN\_U.

KAN_U	2009*	2010	2011	2012	2013**
<i>annual averages</i>					
$T_a$ (°C)	-15.5	-11.6	-18.0	-14.3	-15.4
ambient air pressure (hPa)	799	804	797	800	799
specific humidity (g kg <sup>-1</sup> )	1.5	2.0	1.4	1.9	1.5
wind speed (m s <sup>-1</sup> )	7.0	7.0	6.2	6.5	7.0
albedo	0.85	0.82	0.82	0.79	0.80
<i>summer (JJA) averages</i>					
$T_a$ (°C)	-4.3	-1.8	-2.9	-1.8	-4.5
ambient air pressure (hPa)	809	808	811	811	804
specific humidity (g kg <sup>-1</sup> )	2.9	3.6	3.3	3.7	2.8
wind speed (m s <sup>-1</sup> )	5.3	5.2	5.0	4.6	5.2
albedo	0.78	0.77	0.78	0.71	0.78

\* average 2010–2013 January, February and March

\*\* average 2009–2012 October, November and December

867 Table 4. Surface height changes and mass budgets (measured in winter and calculated in  
868 summer) at KAN U in meters and m w.e., respectively, and ablation duration. The  
869 uncertainty associated with of the surface height change is estimated at to be 0.2 m. The mass  
870 budgets are calculated with an assumed assuming snow density of 360 kg m<sup>-3</sup> (the average  
871 density of the uppermost 0.9 m measured on 26 April 2013), with uncertainty estimated at 40  
872 kg m<sup>-3</sup> (standard deviation among the snow-pit measurements). The snow density assumption  
873 was not needed in 2012 and 2013, when actual density measurements were conducted.

	<u>winter</u> <u>height</u> <u>change</u>	<u>winter</u> <u>budget</u>	<u>summer</u> <u>height</u> <u>change</u>	<u>summer</u> <u>budget</u>	<u>net budget</u>	<u>ablation</u> <u>period</u>
<u>2008–2009</u>	<u>+1.6*</u>	<u>+0.59*±0.15</u>	<u>-0.7</u>	<u>-0.26±0.08</u>	<u>+0.34*±0.12</u>	<u>01/06–</u> <u>19/08</u>
<u>2009–2010</u>	<u>+0.7</u>	<u>+0.25±0.08</u>	<u>-1.2</u>	<u>-0.44±0.09</u>	<u>-0.19±0.12</u>	<u>30/04–</u> <u>05/09</u>
<u>2010–2011</u>	<u>+1.0</u>	<u>+0.37±0.08</u>	<u>-1.1</u>	<u>-0.41±0.09</u>	<u>-0.04±0.12</u>	<u>28/05–</u> <u>13/08</u>
<u>2011–</u> <u>2012**</u>	<u>+0.7</u>	<u>+0.25±0.08</u>	<u>-1.8</u>	<u>-0.86±0.14</u>	<u>-0.61±0.16</u>	<u>27/05–</u> <u>24/08</u>
<u>2012–</u> <u>2013***</u>	<u>+1.2</u>	<u>+0.45±0.09</u>	<u>-0.8</u>	<u>-0.27±0.08</u>	<u>+0.18±0.12</u>	<u>29/05–</u> <u>17/08</u>

\* value inferred from Van de Wal et al. (2012)

\*\* estimate based on snow-pit densities from May 2012

\*\*\* estimate based on snow-pit densities from May 2013

874 Surface mass budgets (measured in winter and calculated in summer) at KAN\_U in m w.e.,  
875 ablation duration and average ablation rates in mm w.e. day<sup>-1</sup> assuming snow density of 360  
876 kg m<sup>-3</sup> (the average density of the uppermost 0.9 m measured on 26 April 2013). This  
877 assumption was not needed in 2012 and 2013 when actual density measurements were  
878 conducted. The uncertainties of the surface height change and snow density are estimated at  
879 0.2 m and 40 kg m<sup>-3</sup>, respectively.

	winter budget	summer budget	net budget	ablation period	average ablation rate
2008–2009	+0.59*±0.15	–0.26±0.08	+0.34*±0.12	01/06–19/08	3.25
2009–2010	+0.25±0.08	–0.44±0.09	–0.19±0.12	30/04–05/09	3.41
2010–2011	+0.37±0.08	–0.41±0.09	–0.04±0.12	28/05–13/08	5.26
2011–2012**	+0.25±0.08	–0.86±0.14	–0.61±0.16	26/05–24/08	9.05
2012–2013***	+0.45±0.09	–0.27±0.08	+0.18±0.12	29/05–17/08	3.33

—\* value inferred from Van de Wal et al. (2012)

—\*\* estimate based on snow pit densities from May 2012

—\*\*\* estimate based on snow pit densities from May 2013

881 Table 5. Annual and summer (June-July-August) average energy fluxes at KAN\_U ( $\text{W m}^{-2}$ ).

	2009*	2010	2011	2012	2013**
<i>annual averages</i>					
$E_S^\downarrow$	155	153	150	145	151
$E_S^\uparrow$	-125	-121	-121	-110	-119
$E_S^{\text{Net}}$	30	32	29	35	32
$E_L^\downarrow$	207	224	205	223	212
$E_L^\uparrow$	-246	-262	-239	-254	-248
$E_L^{\text{Net}}$	-39	-38	-34	-31	-36
$E_R$	-9	-6	-5	4	-4
$E_H$	17	18	12	12	14
$E_E$	-2	-1	-2	-1	-3
$E_G$	-2	-3	1	-2	-2
$E_P$	0.004	0.006	0.009	0.012	0.005
$E_M$	4	8	6	13	5
<i>summer (JJA) averages</i>					
$E_S^\downarrow$	322	305	302	296	313
$E_S^\uparrow$	-252	-234	-236	-208	-242
$E_S^{\text{Net}}$	70	71	66	88	71
$E_L^\downarrow$	237	259	252	260	245
$E_L^\uparrow$	-291	-303	-299	-303	-292
$E_L^{\text{Net}}$	-54	-44	-47	-43	-47
$E_R$	16	27	19	45	24
$E_H$	6	6	8	7	5
$E_E$	-9	-9	-7	-5	-13

---

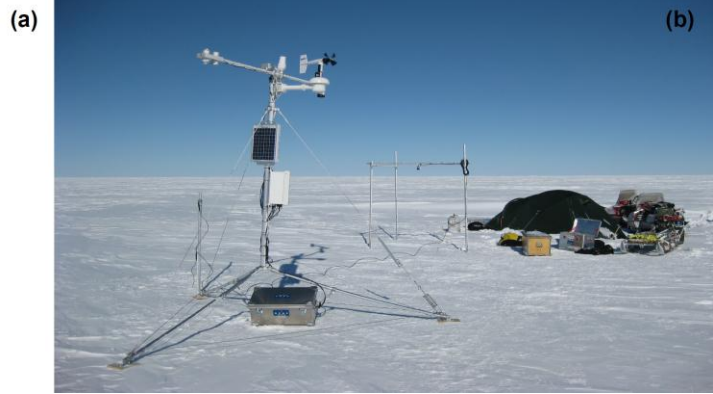
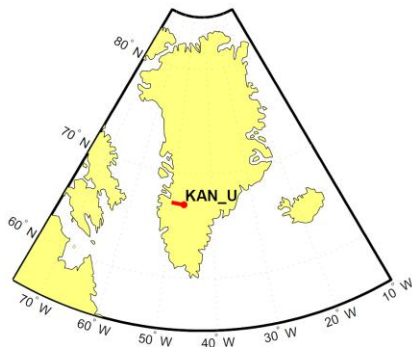
$E_G$	2	4	4	2	1
$E_P$	0.014	0.025	0.035	0.049	0.021
$E_M$	15	28	24	49	17

---

\* used average 2010–2013 values for January, February and March

\*\* used average 2009–2012 values for October, November and December

882

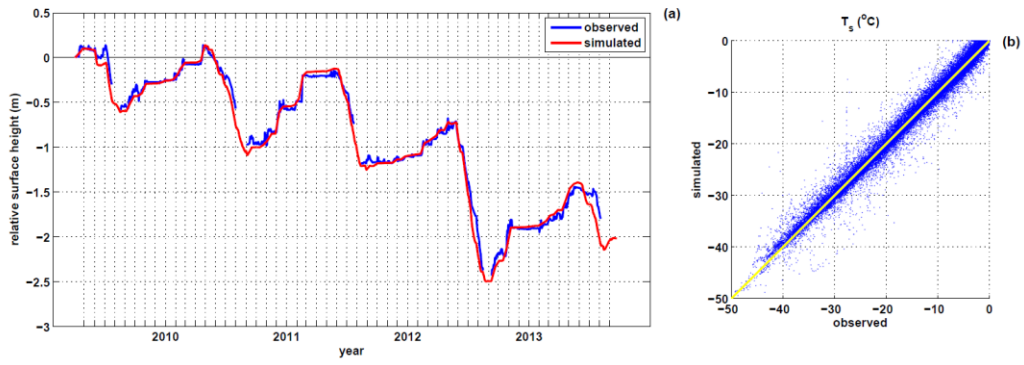


883

884

885 Figure 1. (a) Map of Greenland and the location of KAN\_U. (b) Picture taken after the  
886 installation of KAN\_U (April 2009).

887



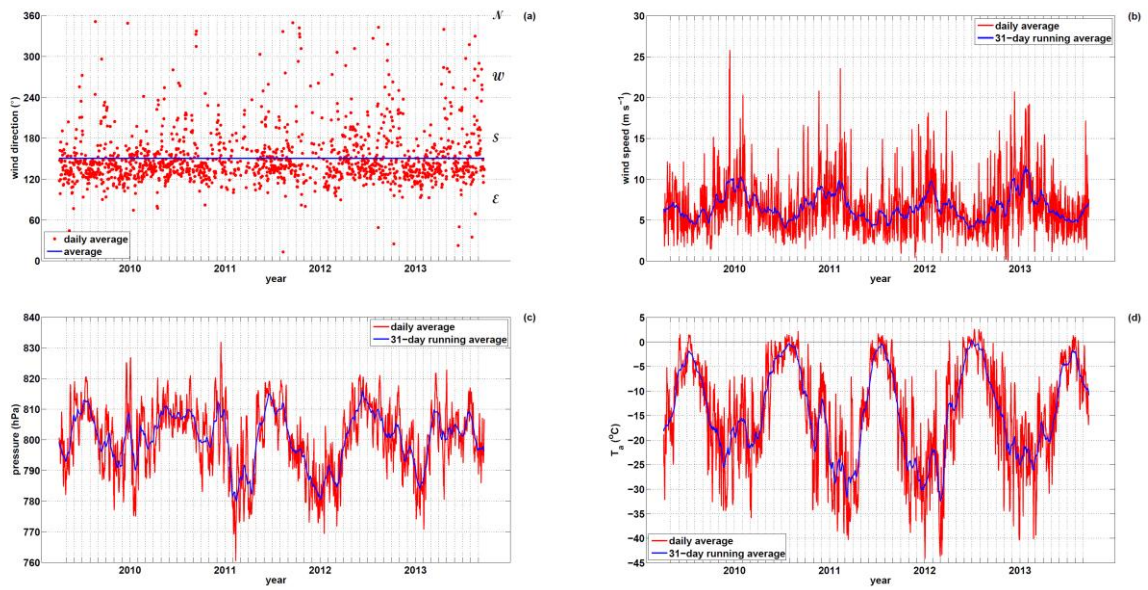
888

889

890 Figure 2. SEB model validation: (a) Observed and simulated relative surface height for the  
 891 period of observations. (b) Observed against simulated  $T_s$  ( $R^2 = 0.98$ ;  $(\Delta T_s)_{\text{avg}} = 0.11$  °C;  
 892 RMSE = 1.43 °C.)

893



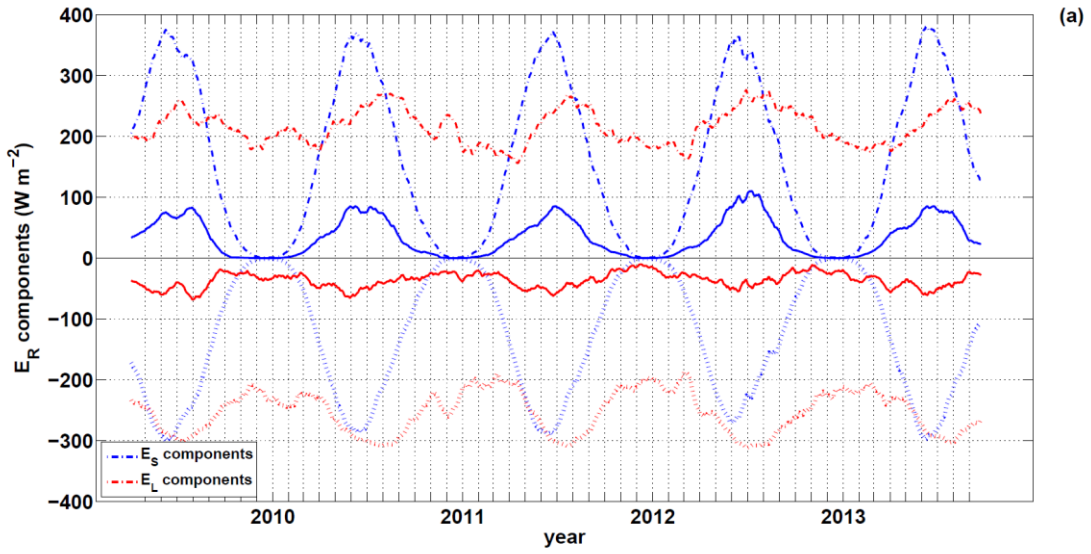


894

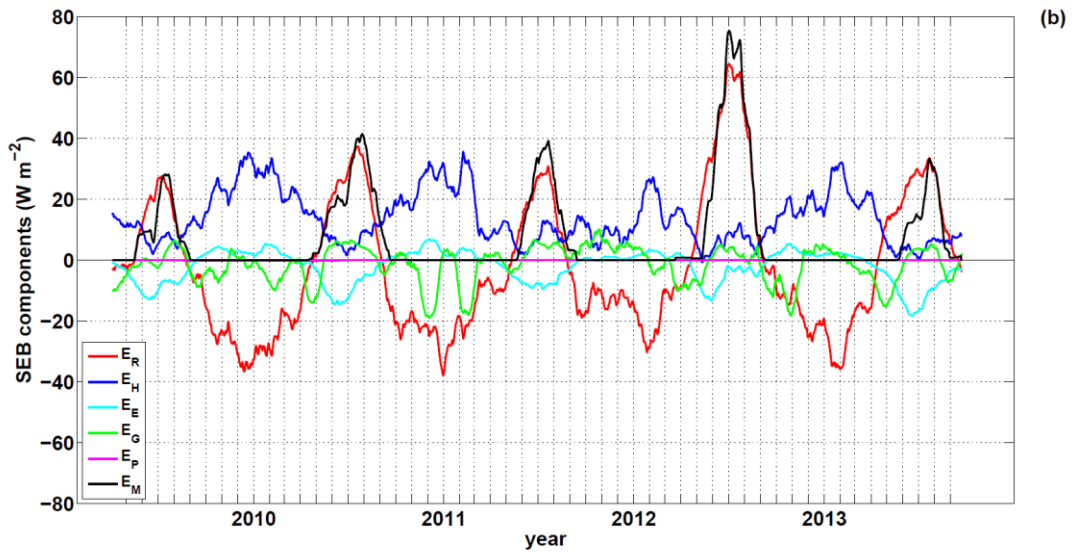
895

896 Figure 3. Average values of: (a) wind direction, (b) wind speed, (c) air pressure and (d) air  
 897 temperature at KAN\_U.

898



899



900

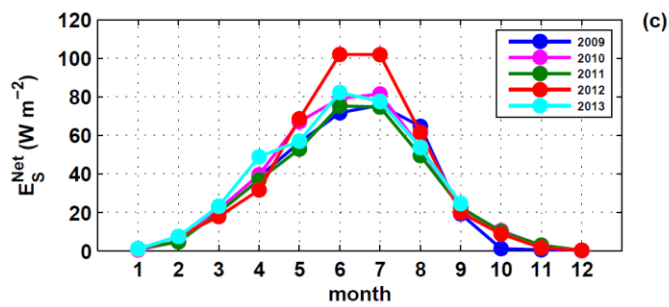
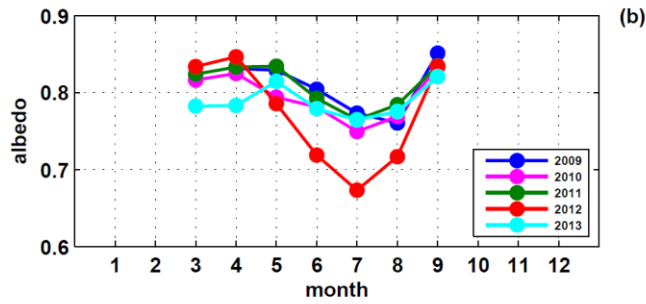
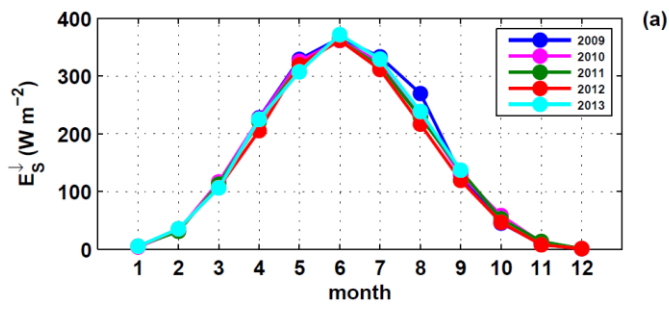
901

902 Figure 4. (a) 31-day running average values of all radiation budget components at KAN\_U.

903 Solid lines indicate the net solar and terrestrial radiation components. (b) Same, as (a), but for

904 all surface energy balance components.

905



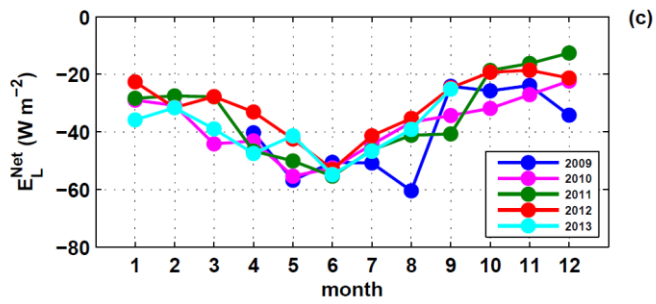
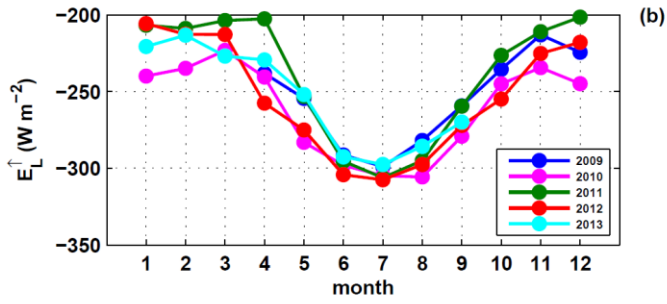
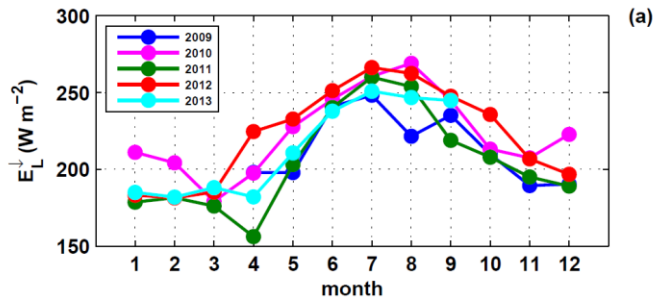
906

907

908 Figure 5. Seasonal cycles for the years 2009–2013 based on monthly averages of: (a)

909 incoming shortwave energy flux, (b) surface albedo and (c) net shortwave energy flux.

910



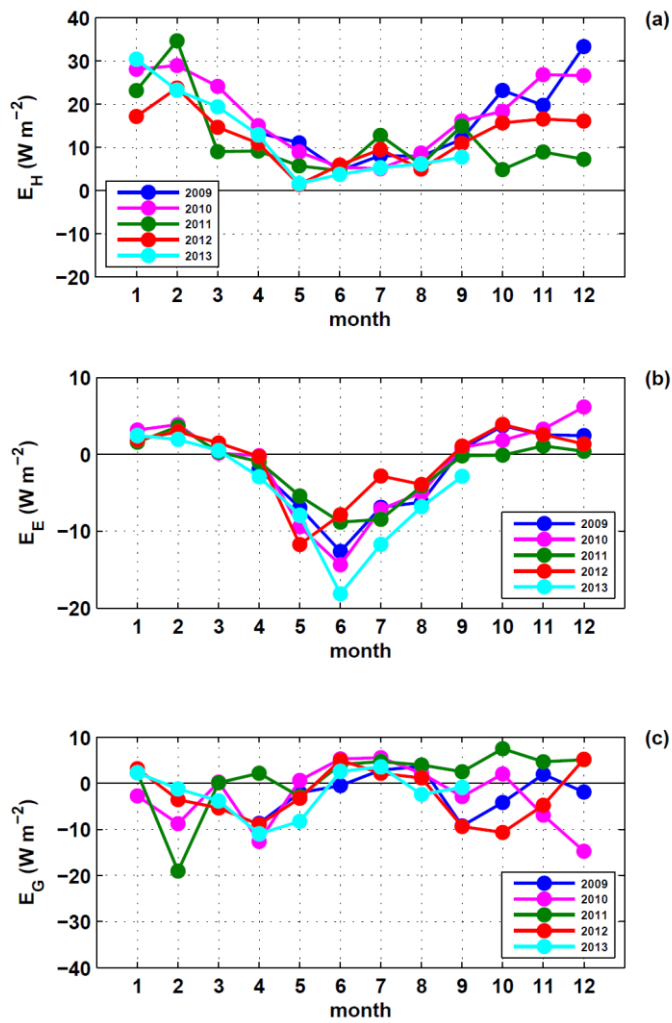
911

912

913 Figure 6. Seasonal cycles for the years 2009–2013 based on monthly averages of: (a)

914 incoming, (b) emitted and (c) net longwave energy flux.

915

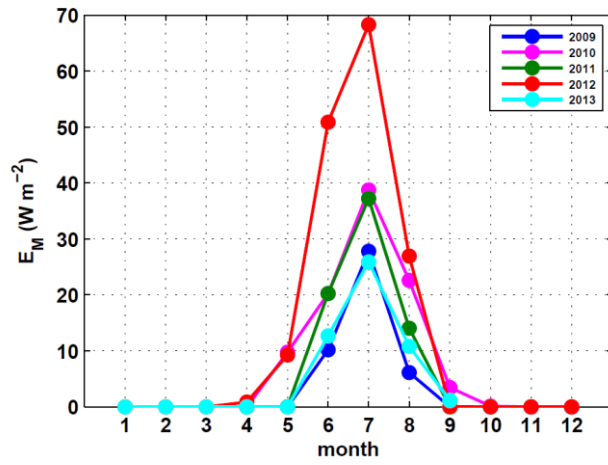


916

917

918 Figure 7. Seasonal cycles for the years 2009–2013 based on monthly averages of: (a) sensible  
 919 heat flux, (b) latent heat flux and (c) subsurface heat flux.

920



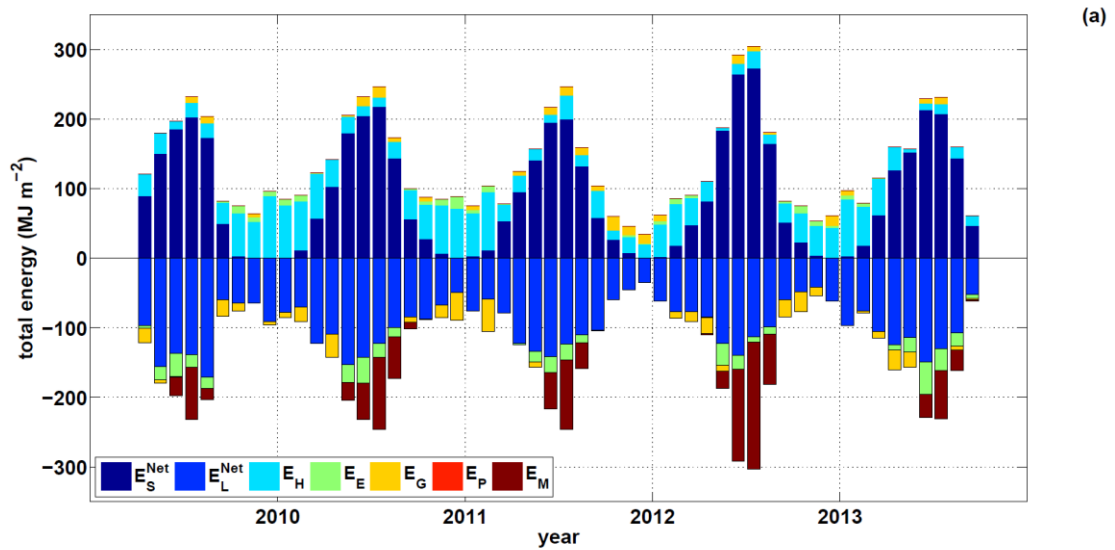
921

922

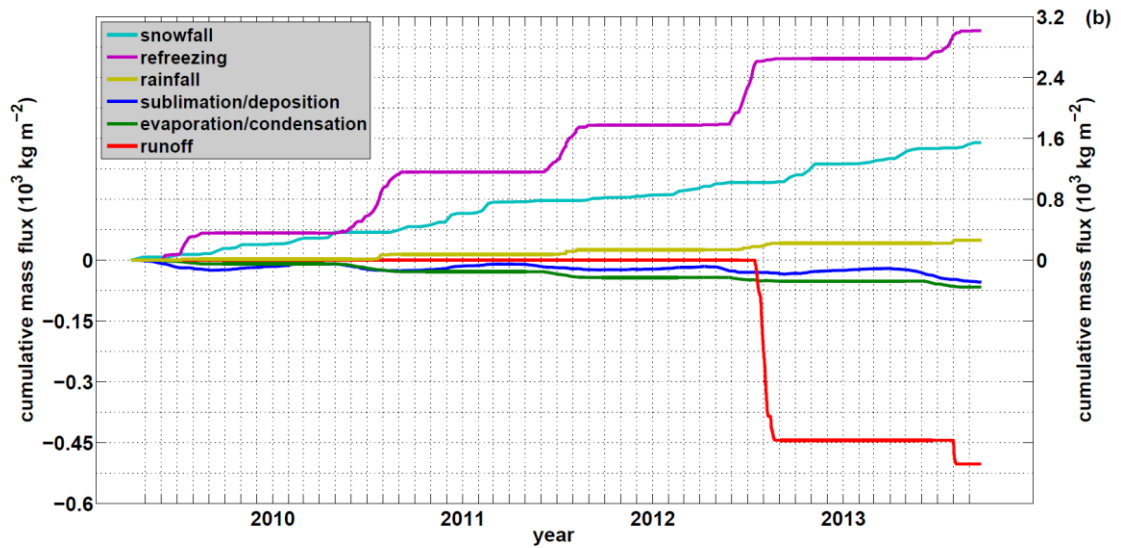
923 Figure 8. Seasonal cycle for the years 2009–2013 based on monthly averages of energy

924 consumed by melt.

925



926

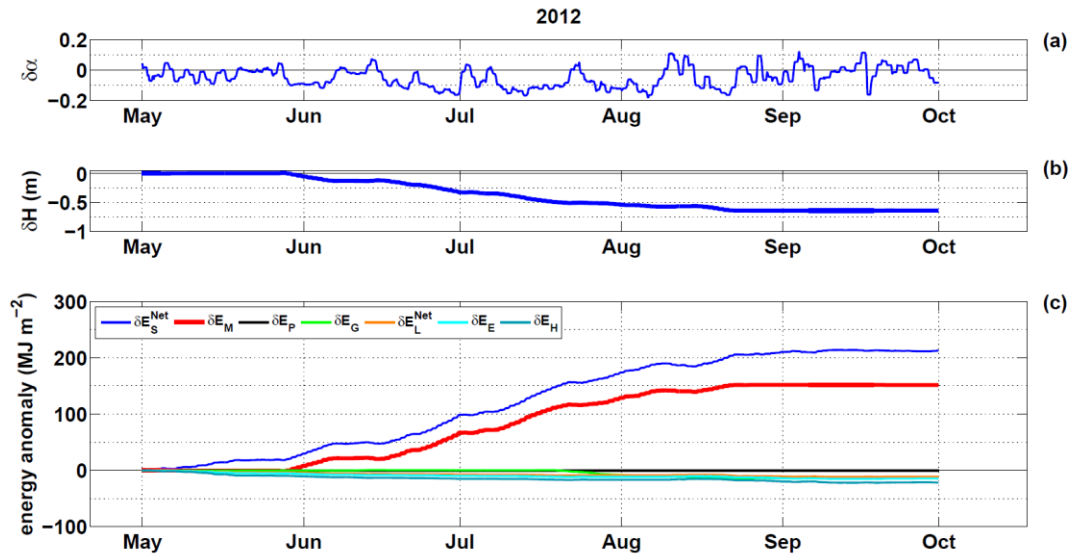


927

928

929 Figure 9. (a) Total energy per unit surface area. (b) Cumulative fluxes of all mass  
 930 components. Note the different y-scales in (b).

931



932

933

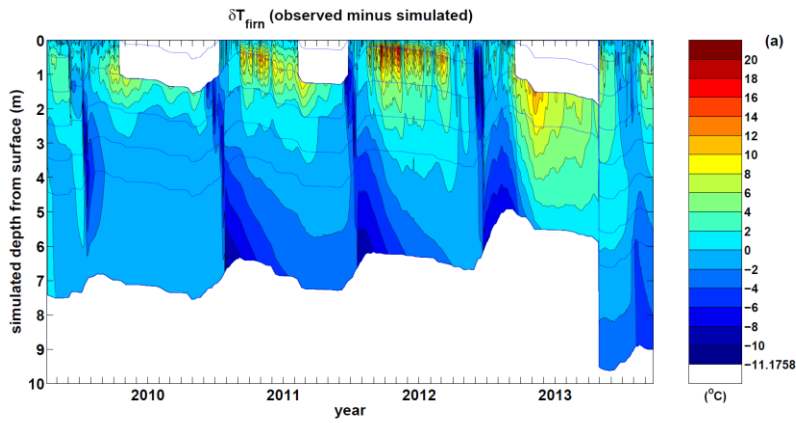
934 Figure 10. (a) 2012 albedo anomaly measured by KAN\_U for the months May–September,

935 (b) simulated relative surface height anomaly and (c) simulated cumulative energy anomalies

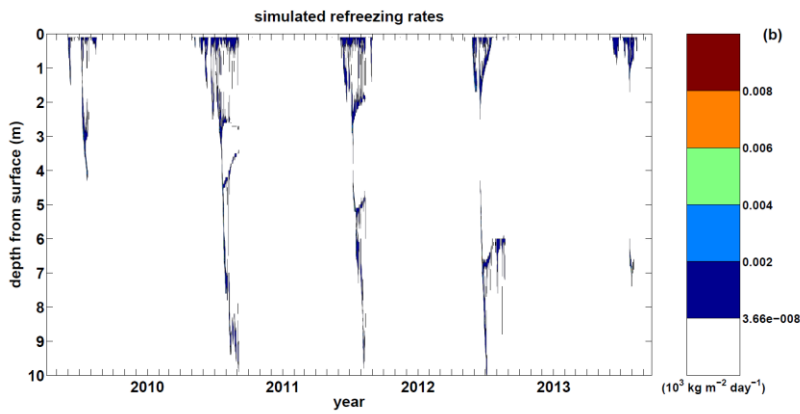
936 for all contributing fluxes.

937

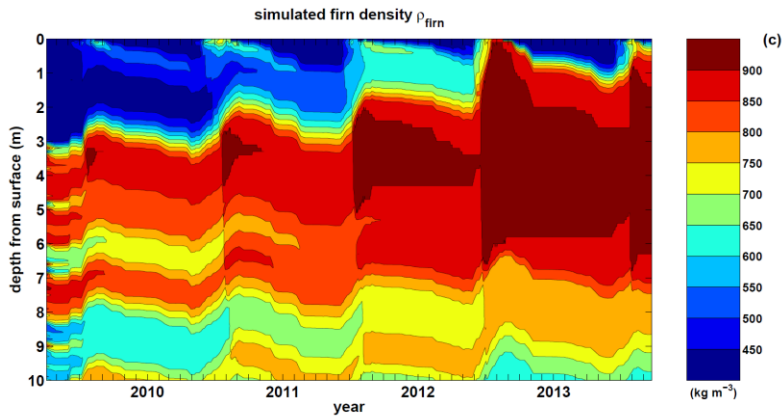




938



939

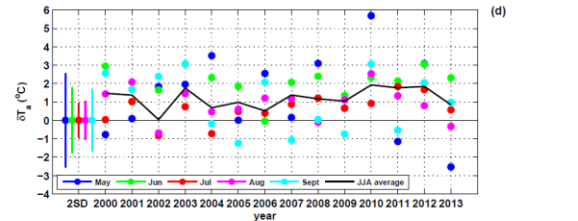
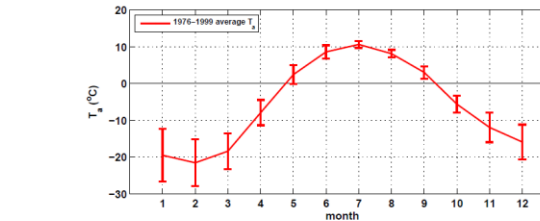
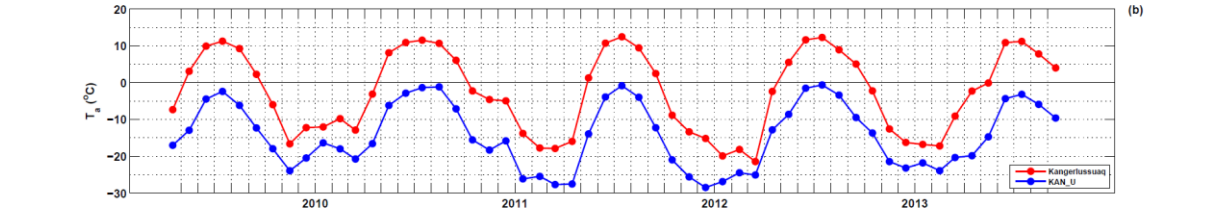
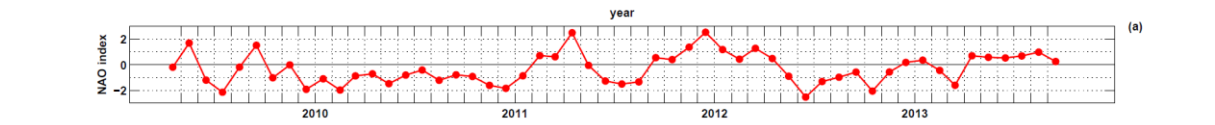
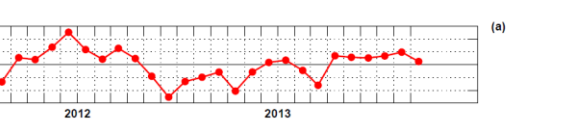
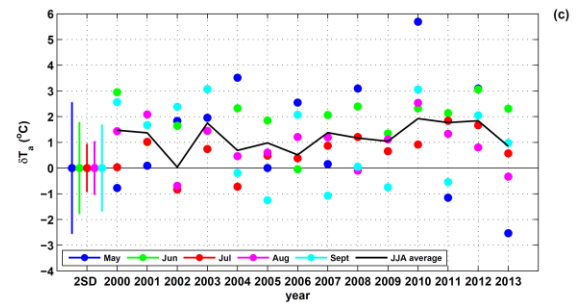
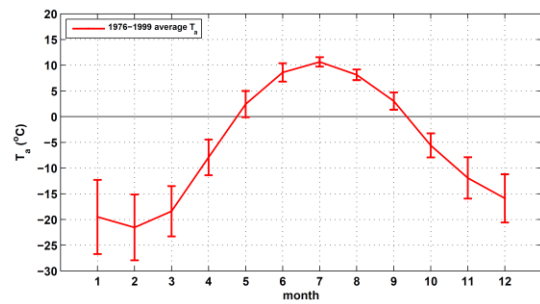
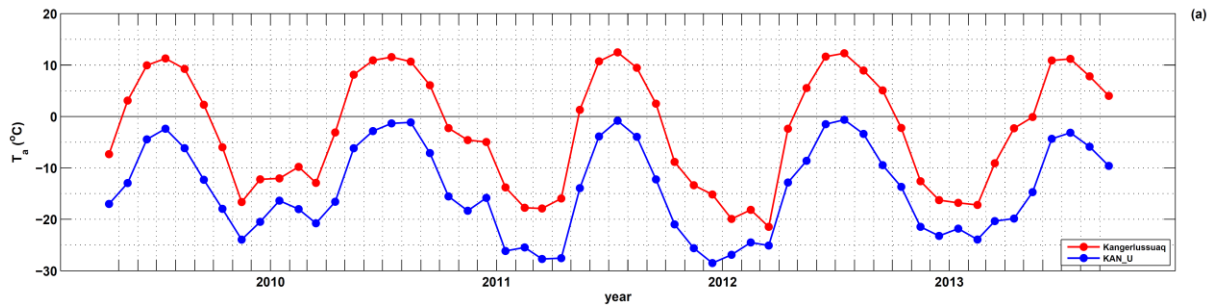


940

941

942 Figure 11. (a) Difference between firn temperature measured by the KAN\_U thermistor string  
 943 and simulated firn temperature. The blue lines indicate the position of the thermistors below  
 944 the surface. The white areas near the surface are due to surfacings thermistors. Note that the  
 945 thermistor string was replaced by a new one drilled on 28 April 2013. (b) Simulated  
 946 refreezing rates. (c) Simulated firn density.

947



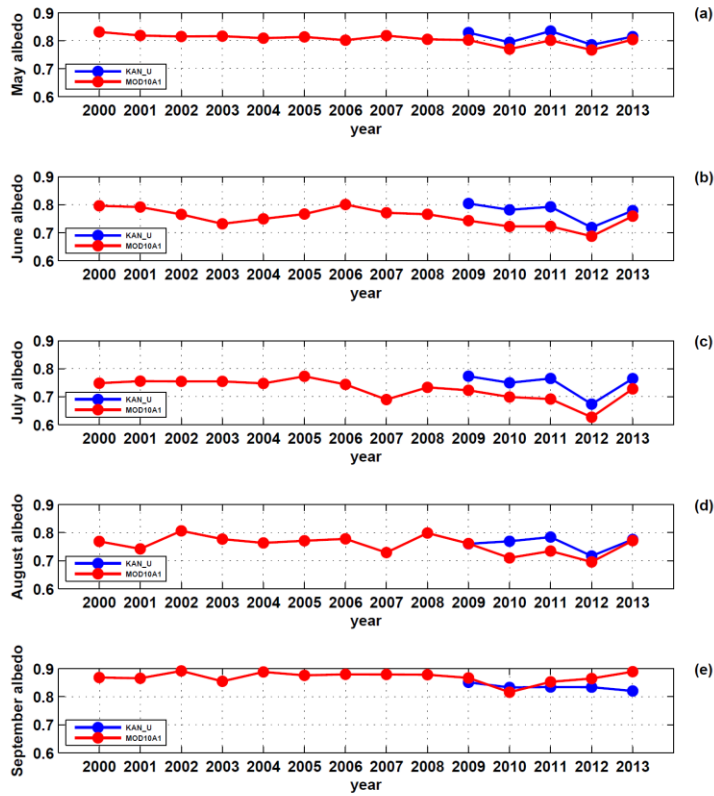
948

949

950

951 Figure 12. (a) Monthly average NAO index. (ab) Monthly air temperature from  
 952 Kangerlussuaq and at KAN U. Correlation coefficients (R): 0.97 for the extent of the KAN\_U  
 953 data, 0.66–0.99 for the months individually, minimum being January. (be) Monthly reference  
 954 period (1976–1999) air temperature at Kangerlussuaq. (ce) Monthly (May to September) and  
 955 summer (June-July-August average) air temperature anomalies at Kangerlussuaq for the years  
 956 2000–2013. Error bars indicate two standard deviations.

957



958

959

960 Figure 13. 11-day Gaussian filtered nearest neighbor 5x5 km MOD10A1 albedo (2000–2013)  
 961 and KAN\_U (2009–2013) albedo for the months: (a) May ( $R = 0.91$ ,  $(\Delta\alpha)_{\text{avg}} = -0.02\text{-m}$ ,  
 962  $\text{RMSD} = 0.02\text{-m}$ ), (b) June ( $R = 0.77$ ,  $(\Delta\alpha)_{\text{avg}} = -0.05\text{-m}$ ,  $\text{RMSD} = 0.05\text{-m}$ ), (c) July ( $R =$   
 963  $0.95$ ,  $(\Delta\alpha)_{\text{avg}} = -0.05\text{-m}$ ,  $\text{RMSD} = 0.05\text{-m}$ ), (d) August ( $R = 0.60$ ,  $(\Delta\alpha)_{\text{avg}} = -0.03\text{-m}$ ,  $\text{RMSD} =$   
 964  $0.04\text{-m}$ ) and (e) September ( $R = -0.19$ ,  $(\Delta\alpha)_{\text{avg}} = 0.02\text{-m}$ ,  $\text{RMSD} = 0.04\text{-m}$ ).